

CHAPTER III
AN OVERVIEW OF SEVERAL RAIN AND
RAIN ATTENUATION MODELS

3.1 INTRODUCTION

3.1.1 Summary of Models

Several models for estimation of the cumulative attenuation statistics on earth-space millimeter paths have been developed. Each of these models appears to have advantages and disadvantages depending on the specific application. In this chapter an attempt is made to briefly summarize the key features of commonly used models. Chapter VI provides information on the application of these models and includes examples. Many of the models employ the concept of "effective path length," which is explained at the end of this chapter.

Table 3.1-1 summarizes the key inputs, outputs and other important features of seven models in their current format. Nearly all of these models are being updated and modified based on recent experimental results and analyses. In addition, other models prepared by major communications companies, such as **Comsat**, are utilized (Gray and **Brown-1979**), but these are **generally** not published in the open literature and are accordingly omitted here.

The models provide rain rate statistics, attenuation statistics? or both. Generally, these statistics can be related by use of the specific attenuation and effective path length relations. (Specific attenuation is described in Chapter II, while the effective path

Table 3.1-1. Summary of Model Parameters

Model	Inputs	outputs	Comments
Rice-Homberg	Climate or Site-Specific Mean Annual Rainfall plus Ratio of Thunderstorm-to-Total Rain.	Cumulative Time Distribution of Rainfall.	Two Rain Modes Considered: Thunderstorm & Uniform Rains. Probability of Rain Rate Exceedance for Either or Both Modes is Available.
Dutton-Dougherty	Same as Rice-Homberg and Link Parameters (e.g., Frequency, Elevation Angle).	Rain or Gaseous Attenuation Associated with a Given Exceedance Time Percentage.	Utilizes Modified Rice-Holmberg Rain Model. Provides Confidence Limits, Given Two Additional Rain Rate Distributions.
Global	Location and Link Parameters.	Rain Attenuation Associated with a Given Exceedance Time Percentage.	All Rain Attenuation Parameter Values are Selfcontained. Globally Applicable.
Two-Component	Same as Global.	Exceedance Time Percentage Associated with a Given Rain Attenuation.	Same Rain Model (& Comments) as for Global Model. Two Rain Modes Considered: Convective Cell and Debris Rains.
CCIR	Same as Global.	Rain Attenuation Associated with a Given Exceedance Time Percentage.	All Rain Attenuation Parameter Values are Selfcontained. Globally Applicable.
Lin	Five Minute Rain Rate and Link Parameters.	Attenuation Associated with a Given Rain Rate.	Simple Extension of Terrestrial Path Rain Attenuation Model.
Simple Attenuation (SAM)	Rain Statistics and Link Parameters.	Attenuation Associated with a Given Rain Rate.	Assumes Exponential Shaped Rain Profile.

length concept is summarized at the end of this chapter.) For example, the **Rice-Holmberg** model only computes the exceedance probability statistics for rain rate, but this is relatable to attenuation by use of the specific attenuation and the effective path length. The Dutton-Dougherty, **CCIR**, Two-Component, and Global models provide the attenuation statistics given the geographic and link parameters. That is, they give the rain rate statistics within the model.

3.1.2 Concepts of Rainfall Statistics

3.1.2.1 Cumulative Statistics. The cumulative statistics for either rain rate or attenuation are usually presented as the probability of exceedance (abscissa) versus the rain rate or attenuation (ordinate). They represent stable statistics averaged over a period sufficiently long that variations in the lowest frequency component of the time distribution are averaged. For rain rate and rain attenuation the period corresponding to the lowest frequency is generally considered to be one year. Higher frequency components are the seasonal and daily variation of the rain rate. For example, in the eastern US, the higher frequency components arise because more rain falls in the summer than in the winter, and more rain falls between noon and 6 PM than between 6 AM and noon local time. **Some** people have suggested that the n-year solar cycle is the lowest frequency component, but this has not been observed by the Weather Service.

Based on the above considerations the cumulative statistics for several years are required before "stable" annual statistics are obtained. For this reason, experimentally generated data bases for both rain and attenuation are not generally good until 5 or 10 years of data are included. However, because of the limited lifetime of the beacon satellites, attenuation data at a known frequency and elevation angle is generally not available for this length of period (**Kaul et al-1977**). Therefore data from several satellites launched over a long period are required. Since they are not at the same frequency and elevation angle, these results must be scaled in order

to be combined. Frequently this process has not been done accurately, resulting in small segments of attenuation data which are not representative of the long term statistics.

Based on the above discussions it appears that the only present recourse is to utilize rain rate data as derivable from Weather Bureau or other long-term measurements. This leads to the exceedance curves or rain rate. The attenuation is then derived from the relations between rain rate and attenuation.

3.1.2.2 Outage Period Statistics. System designers are also interested in the average length of time a given threshold of rain rate or attenuation is exceeded (also termed the outage time). In addition, the distribution of the outage time about the average is desired. Theoretical work of Lin (1973) has shown that the distribution is approximately **lognormal**.

Besides the outage time, Hyde (1979) has identified the desire to know the average time between outage periods within a given rain event, and the average time between outages between two rain events. The first case recognizes that outages may occur several times during the same general rain event because the rain rate is highly variable during an event. For example, the passage of several rain cells associated with a given rain front may cause several outages as each cell dominates the path attenuation. It is desirable to know the approximate period between these outages and the distribution of these outage periods as a function of attenuation threshold and type of rain event. This type of data is expected to be dependent on the geographic region because the weather fronts are distorted by the presence of mountain ranges, lakes, cities, etc. Therefore, extrapolation to other regions is difficult unless their weather systems are similar.

The second case (average time between outages in two rain events) correlates the period between severe storms in a given region. This period is expected to be seasonally dependent because in most regions the high rain rate storms usually occur during a

short period of the year. Again, some statistical estimate of the average period and the distribution of the periods would be desirable.

-Generally, outage period data is not as readily available as the cumulative attenuation statistics data. Therefore, the designer must rely on the limited data bases available from CCIR (1986, Rpt 564-3), Comsat (Rogers and Hyde-1979) or Lin (1973, 1980). Vogel (1982) has calculated time-between fade (intermission) statistics for 19 and 28 GHz at Austin, Texas. An estimate of the upper limit of the outage time is presented in Chapter VI.

3.2 RICE-HOLMBERG MODEL

3.2.1 Types of Storms

The **Rice-Holmberg** (R-H) Model (Rice and **Holmberg-1973**) is based upon two rainfall types: convective ("Mode 1", thunderstorm) rains and stratiform ("Mode 2", uniform) rains. The statistical model is based upon the sums of individual exponential modes of rainfall rates, each with a characteristic average rate R. According to this descriptive analysis

$$\text{rainfall} = \text{Mode 1 rain} + \text{Mode 2 rain}$$

The exponential distribution chosen to describe "Mode 1 rain" corresponds to a physical analysis of **thunderstorms**, while "Mode 2 rain," represented by the sum of two exponential distributions is all other rain. In temperate climates only convective storms associated with strong updrafts, high radar tops, hail aloft and usually with thunder can produce the high rainfall rates identified by Mode 1. Only the highest rates from excessive precipitation data are used to determine parameters for Mode 1, which is intended to represent a physical mechanism as well as a particular mathematical form.

3.2.2 Sources of Data

The rainfall statistics in the R-H model are based upon the following:

- 1) Average year cumulative distributions of hourly rates for the 10 years 1951 to 1960 and for a total of 63 stations, with 49 in the continental U.S. as summarized in the Weather Service **Climatological** Data for this period;
- 2) Distributions for 15-year averages with recording intervals of **6, 12, and 24 h** for 22 of these stations (**Jorgenson, et al-1969**);
- 3) Accumulations of short-duration excessive precipitation for 1951 to 1960 for recording intervals of **5, 10, 15, 20, 30, 45, 60, 80, 100, 120, and 180 min** for 48 U.S. stations;
- 4) A U.S. map of the highest 5-rein rates expected in a two-year period (**Skerjanec and Samson-1970**);
- 5) Maximum monthly rainfall accumulations and the average annual number of thunderstorm days for the period 1931 to 1960 for 17 U.S. stations and 135 additional stations reported by the World Meteorological Organization.

3.2.3 R-H Model Parameters

The average annual total rainfall depth M is the sum of contributions M_1 and M_2 from the two modes:

$$M = M_1 + M_2 \text{ mm} \quad (3.2-1)$$

and the ratio of "thunderstorm rain" M_1 to total rain M is defined as

$$\beta = M_1/M \quad (3.2-2)$$

The number of hours of rainy t-rein periods for which a surface point rainfall rate R is exceeded is the sum of contributions from the two modes:

$$T_t(R) = T_{1t} q_{1t}(R) + T_{2t} q_{2t}(R) \text{ hours}$$

There are 8766 hours per year, so $T_t(R)/87.66$ is the percentage of an average year during which t-rein average rainfall rates exceed R

mm/h . The data show that the average annual clock t-rein rainfall rate for each of the modes is fairly constant. On the other hand, the total number of rainy t-rein periods for each mode is relatively much more variable from year-to-year and between stations or climate regions. Rainfall climates defined by Barry and Chorley (1970) for the United States were found to correspond very well with observed regional variations of the parameter β .

The average annual total of t-rein periods of Mode 1 and Mode 2 rainfall are T_{1t} and T_{2t} , respectively. The average annual Mode 1 and Mode 2 rainfall rates are therefore

$$\begin{aligned}\bar{R}_{1t} &= M_1/T_{1t} \text{ mm/h} \\ \bar{R}_{2t} &= M_2/T_{2t} \text{ mm/h}\end{aligned}\tag{3.2-3}$$

Note that M_1 and M_2 are not functions of t, since the amount of rainfall collected over a long period of time does not depend on the short-term recording interval t. But the total number of hours T_{1t} or T_{2t} of rainy t-rein intervals (collecting at least 0.01 in or 0.254 mm of rain per interval) will depend on t.

The factors $q_{1t}(R)$ and $q_{2t}(R)$ are the complements of cumulative probability distributions. Each factor is the number of hours that a rate R is exceeded by Mode 1 or Mode 2 rain divided by the total number of hours, T_{1t} or T_{2t} , that there is more than 0.254 mm of rain in a t-rein period.

3.2.4 Time Intervals

The formulas to be presented are for $t=1$ clock-minute rates. Here clock-minutes are defined as beginning "on the minute" for a continuous t-minute period.

For the more general case where $t>1$ rein, one more prediction parameter is required in addition to the two that have been defined as M and B. This additional parameter is the number of hours of

rain per year, D. The formulas proposed here for $q_{1t}(R)$ and $q_{2t}(R)$ assume that the number of rainy days in an average year is

$$D/24 = 1 + M/8 \text{ rainy days} \quad (3.2-4)$$

where D is in hours and M is in millimeters. This relation has been found good, on the average, for continental U.S. stations. A comparison of the cumulative distributions versus the surface rainfall rate R for various values of t from 1 minute to 1 day is shown in Figure 3.2-1. Clearly, for $\beta=0.125$ and $M=1000\text{mm}$, the values for t=1 and 5 minutes are nearly equal, but longer periods give a significantly different value for $T_t(R)$.

3.2.5 Model Results for One-Minute Intervals

For t=1, the more general formulas are almost independent of D, so that

$$\begin{aligned} q_{1t}(R) &= \exp(-\bar{R}/R_{1t}) \\ q_{2t}(R) &= 0.35 \exp(-0.453074 R/R_{2t}) \\ &+ 0.65 \exp(-2.857143 R/\bar{R}_{2t}) \end{aligned} \quad (3.2-5)$$

and the annual average Mode 1 and Mode 2 rates \bar{R}_{1t} and \bar{R}_{2t} are very nearly equal to 33.333 and 1.755505 mm/h, respectively. Then $T_1(R)$ may be written as

$$\begin{aligned} T_1(R) &= M \{ 0.03 \beta \exp(-0.030R) + 0.21(1-\beta) [\exp(0.258R) \\ &+ 1.86 \exp(-1.63R)] \} h. \end{aligned} \quad (3.2-6)$$

Use of this relation allows normalized cumulative time distributions to be calculated. Figure 3.2-2 is an example of this result for t=1 minute and B values from 0 to 0.75. Typical values for B and M throughout the US and Canada are given in Figures 3.2-3 and 3.2-4, respectively. Note that the values quoted in Figure 3.2-4 are in inches rather than millimeters required for M. Rice

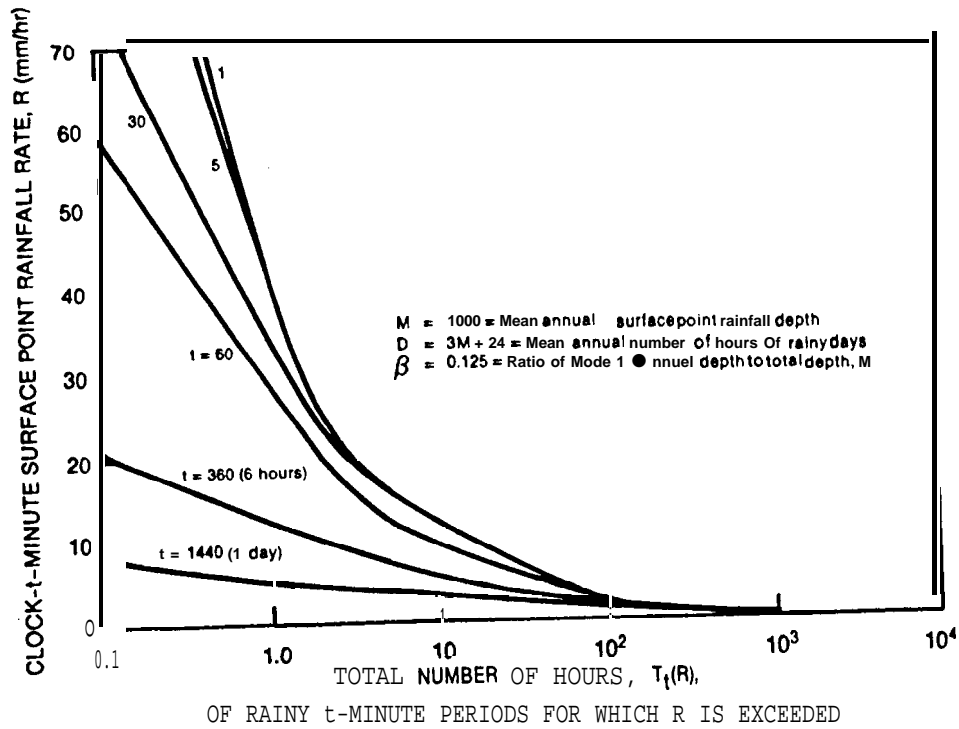


Figure 3.2-1. Average Year Cumulative Time Distributions

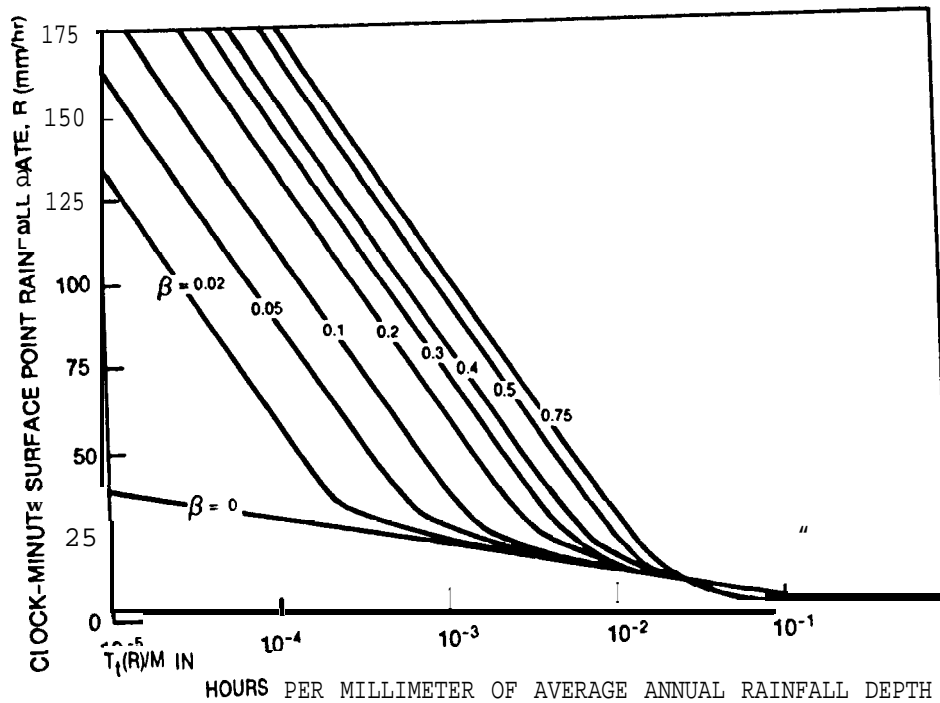


Figure 3.2-2. Normalized Cumulative Time Distributions

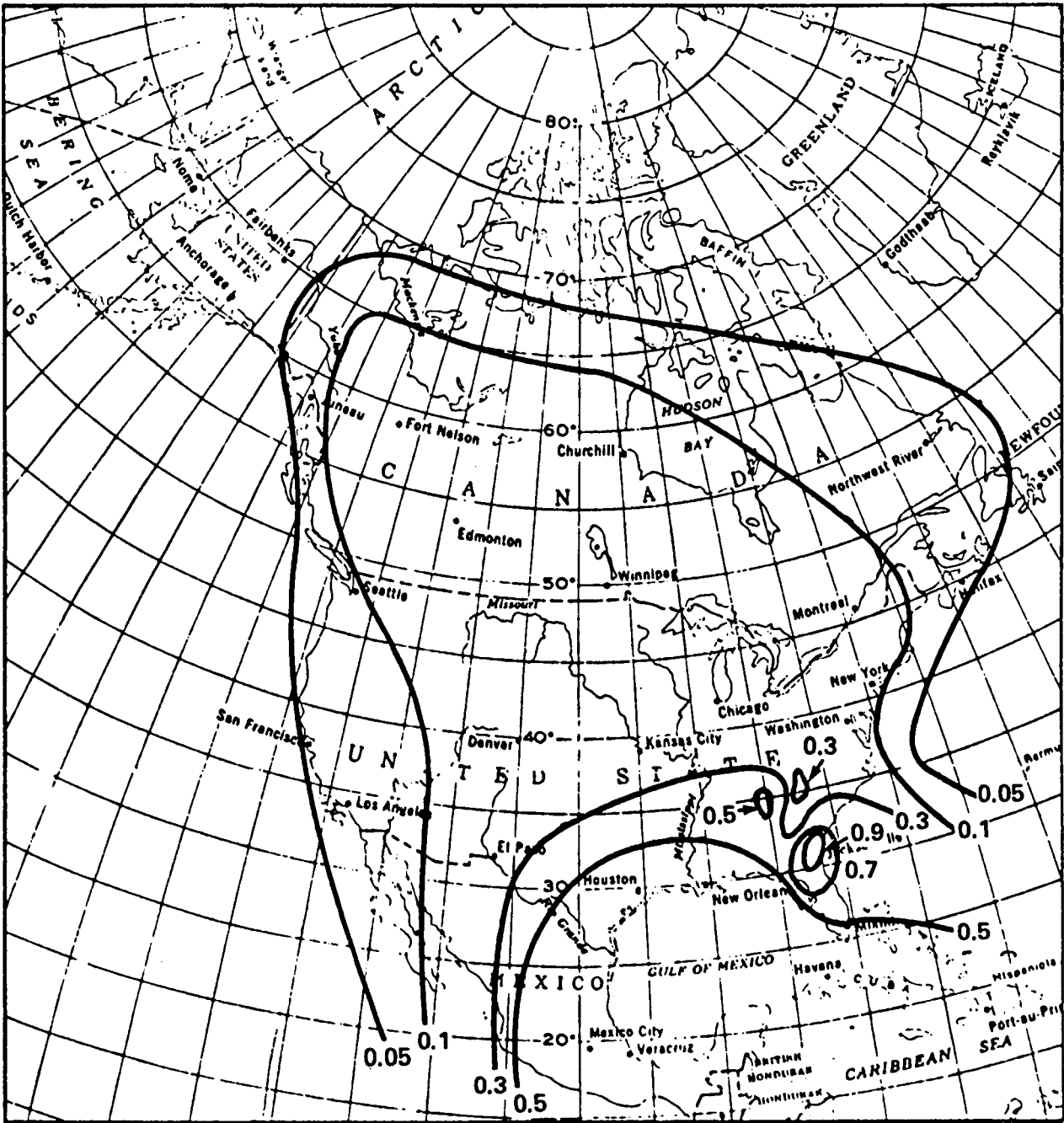


Figure 3.2-3. The Parameter β in the Rice-Holmberg Model Over the U.S. and Canada

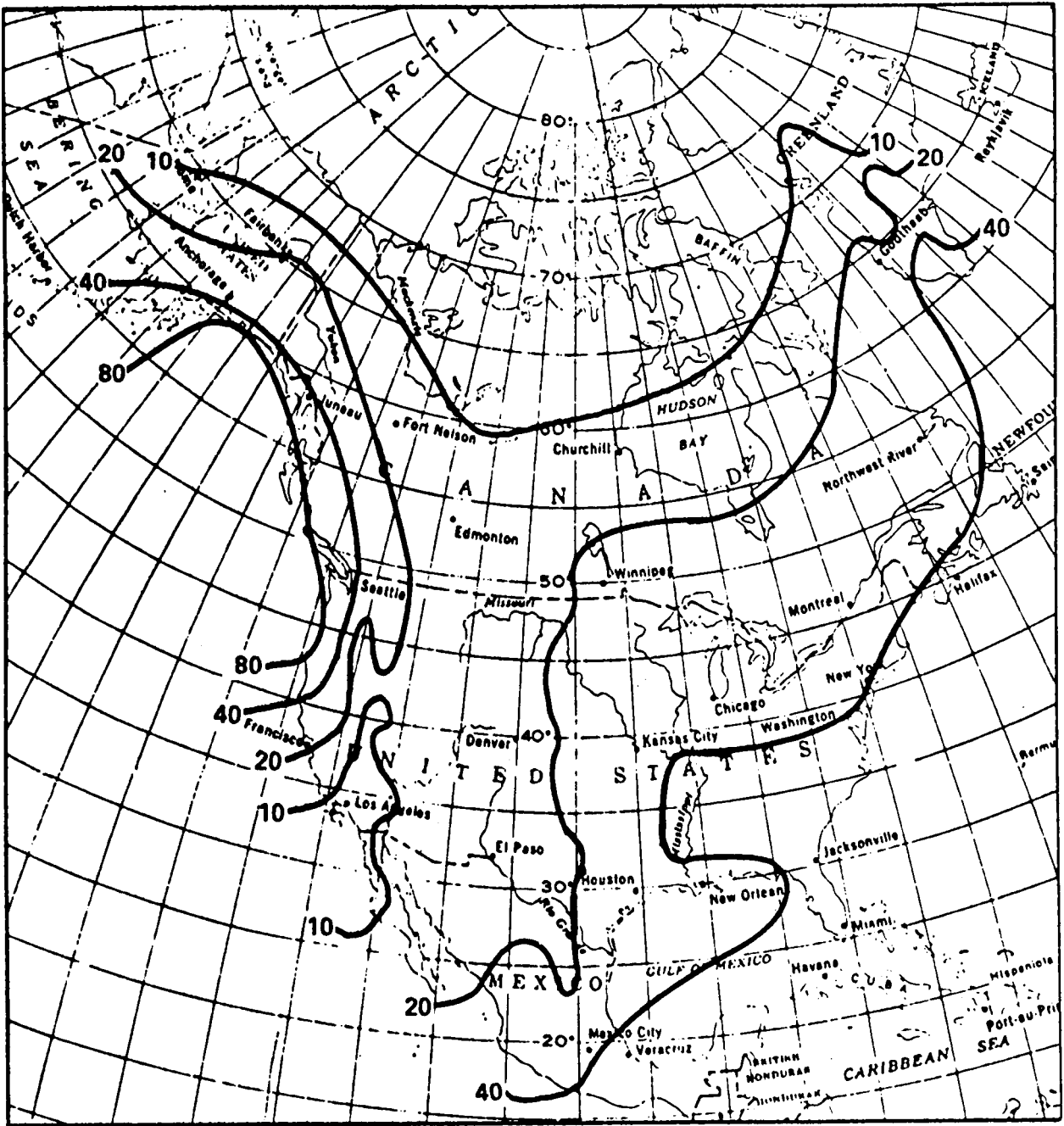


Figure 3.2-4. Mean Annual Precipitation in Inches in U.S. and Canada (1 inch = 25.4 mm)

and **Holmberg** (1973) have also presented values throughout the world in their original article.

Dutton and Dougherty (1979), (1984), provided a less cumbersome version of the R-H model by fitting relatively simple formulations to various parts of the R-H distribution curve. This "modified **Rice-Holmberg** model" was applied to a data base of 304 geographically diverse, data intensive locations in the U.S., (including Alaska and Hawaii), and year to year standard deviations of rain rate were developed. The results showed a marked improvement in the bounds of prediction? which appear to encompass the measured data more completely.

These same authors also extended the R-H rain-rate distribution to include a direct prediction of attenuation distributions for specified paths and locations. This attenuation prediction model is the subject of the next section.

3.3 DUTTON-DOUGHERTY MODEL

The Dutton-Dougherty (DD) Model (**Dutton** and Dougherty-1973, **Dutton-1977**; Dutton, Kobayashi, and Dougherty-1982) includes attenuation due to both rain and gases. The rainfall rate distributions it uses are based on a series of modifications to the **Rice-Holmberg** Model (**Dutton**, et al-1974). The DD Model has been incorporated into a computer program which is available to users from the National Telecommunications and Information Administration. The DD rain and attenuation model components are described separately below.

3.3.1 DD Rain Characterization

The modified **Rice-Holmberg** (R-H) Model, as used in the DD Model, determines the number of hours of rainy t-minute periods, $T_t(R)$, for which a surface rain rate, R, is expected to be exceeded. The value $T_t(R)$ is given in the modified R-H model as

$$T_t(R) = \begin{cases} T_{1t} \exp(-R/\bar{R}_{1t}) & R \geq R_c \\ (T_{1t} + T_{2t}) \exp(-R/R_t') & R < R_c \end{cases} \quad (3.3-1)$$

with

$$T_{1t} = \beta M / \bar{R}_{1t} \text{ hours} \quad (3.3-2)$$

$$T_{2t} = (1 - \beta) M / \bar{R}_{2t} \text{ hours} \quad (3.3-3)$$

Where R_c is a "crossover" rain rate between a convective mode of rainfall ($R \geq R_c$) and stratiform mode of rainfall ($R < R_c$) and other parameters are defined in the R-H Model description. R_t' is a new parameter not used in the R-H Model. This biexponential representation of $T_t(R)$ is strictly analogous to the rainfall conceptions of Rice and Holmberg (1973). From (3.3-1), R_c can be evaluated by setting

$$T_{1t} \exp(-R_c/\bar{R}_{1t}) = (T_{1t} + T_{2t}) \exp(-R_c/R_t') \quad (3.3-4)$$

because it represents the intersection of the two curves in (3.3-1). Thus, we obtain

$$R_c = \bar{R}_{1t} R_t' / (\bar{R}_{1t} - R_t') \ln[(T_{1t} + T_{2t}) / T_{1t}] \quad (3.3-5)$$

The modified R-H model uses direct estimation of T_{1t} , T_{2t} , R_{1t} , and R_t' from M , β , and D . This was achieved by using a multiple linear regression to obtain a best fit of T_{2t} , \bar{R}_{1t} , and R_t' in terms of the parameters M , β , and D . It was not necessary to fit T_{1t} , since it is given very simply in terms of M , β , and \bar{R}_{1t} by (3.3-2). The resulting best fits were of the form

$$\bar{R}_{1t} = a_{1t}M + a_{2t}\beta + a_{3t}D + a_{4t} \pm S_1 \quad (3.3-6)$$

$$T_{2t} = b_{1t}M + b_{2t} \pm S_2 \quad (3.3-7)$$

$$R_t = b_{3t}M + b_{4t}\beta + b_{5t}D + b_{6t} \pm S_3 \quad (3.3-8)$$

where the coefficients are $a_{1t} \dots a_{4t}$ and $b_{1t} \dots b_{6t}$, and the sample standard errors of estimate are $S_1 \dots S_3$.

The third modification is to the portion of the distribution that lies between the rainfall rates of 5 and 30 mm/hour, since two difficulties arise if the equation (3.3-1) is used exclusively for the entire distribution:

- 1) the transition between curves at R_c is decidedly not smooth, and
- 2) predictions via (3.3-1) can be noted to be as much as 50 percent below the R-H model in the same vicinity.

In order to partially alleviate these difficulties? it was arbitrarily determined that

$$T_t(R) = T_{st} \exp(-\sqrt[4]{R/R_{st}}) \quad (3.3-9)$$

could be reasonably fit to the data, with proper curvature and simplicity, for $1 \leq t \leq 60$ min and $5 \leq R \leq 30$ mm/hour.

For $t > 60$ min (i.e., $t=360, 1440$ rein), the formulation (3.3-1) fits the R-H model sufficiently well over the entire rain rate distribution for operational purposes, so that no additional modification of (3.3-1) is necessary. In summary, then, the resultant modification of the R-H model is:

$$T_t(R) = \begin{cases} T_{1t} \exp(-R/\bar{R}_{1t}) & R > 30 \text{ mm/h} \\ (T_{st} \exp(-\sqrt[4]{R/R_{st}})) & 5 \text{ mm/h} \leq R \leq 30 \text{ mm/h} \\ (T_{it} + T_{2t}) \exp(-R/R_t') & R < 5 \text{ mm/h} \end{cases} \quad (3.3-10)$$

for $1 \text{ min} \leq t \leq 60 \text{ min}$. and

$$T_t(R) = \begin{cases} T_{1t} \exp(-R/\bar{R}_{1t}) & R \geq R_c \\ (T_{it} + T_{2t}) \exp(-R/R_t') & R < R_c \end{cases} \quad (3.3-11)$$

for $t > 60$ min.

3.3.2 Attenuation Prediction in the DD Model

Dutton (1977) has estimated the variance and confidence levels of the rain rate prediction, and Dougherty and Dutton (1978) have estimated the year-to-year variability of rainfall within a given rain zone. The DD Model attenuation prediction range now extends to 0.001 percent of a year.

Extending the rain model to include attenuation on earth-space paths, Dutton (1977) has assumed the Marshall and Palmer (1948) raindrop distribution. He has also included some degree of modeling of rainfall in the horizontal direction. This is achieved by means of what is termed the "probability modification factor" on earth-space links.

The probability modification factor, F , is given by

$$F \cong \frac{(f/15)^2}{A(f,\theta)} (0.2740 + 0.987) \quad (3.3-12)$$

the factor cannot exceed unity, however. In (3.3-12), f is the frequency in GHz, θ is the elevation angle to the satellite in degrees, and $A(f,\theta)$ is the path attenuation in dB. The form was derived from rain storm cell size data given in a particularly useful form by Rogers (1972). The Rogers data, however, were all taken in the vicinity of Montreal, Canada. It would be desirable to have more globally diverse data in order to provide a basis for a more general probability modification factor.

The probability modification factor, applied strictly to attenuation, multiplies the percent of time, P , during an average year that a point rainfall rate is expected at a given location. The multiplied value represents the percent of time, P , ($P \leq P_0$), that attenuation corresponding to R is expected along the path to a

satellite. In effect, a point-to-path rain rate conversion accounting for horizontal inhomogeneity is accomplished.

The probability modification factor given by (3.3-12) applies for exceedance percentages down to 0.01% of a year. The **DD** model has been extended (Dutton, et al - 1982) to 0.001% of a year by both empirical and analytical means. The empirical extension is simply to make the probability modification factor at 0.001% equal to the value at 0.01%:

$$F(0.001\%) = F(0.01\%) \quad (3.3-13)$$

The analytical extension gives essentially identical results. The extensions recognize that the nature of the very heavy convective rains occurring on the order of 0.001% of the time is different from that of the more "routine" rains of the 0.1% to 0.01% regime.

In the **DD** model the surface rainfall rate is translated into liquid water content per unit volume, L_0 , measured at the ground. The liquid water content at some height, h , above the ground, $L(h)$, can be modeled as a function of L_0 (Dutton - 1971). The modeling of $L(h)$ is different for the **stratiform** and convective rain systems. In the **stratiform** modeling $L(h)$ is assumed constant to the rain-cloud base, then decreases to zero at the storm top height H . In the convective modeling $L(h)$ increases slightly to the rain-cloud base and then decreases to zero at H , the storm top height.

Attenuation per unit length, $a(f, h)$, due to rain can be calculated from $L(h)$ via expressions of the form

$$a(f, h) = c(f) [L(h)]^{d(f)} \quad (3.3-14)$$

using the data of Crane (1966). Hence, the distinction between the **Rayleigh** region ($f < 10$ GHz, approximately) and the Mie region ($f > 10$ GHz) is implicit, because the coefficients $c(f)$ and $d(f)$ are frequency dependent. In the **Rayleigh** region, it can be shown that $d(f)=1$. An interpolation scheme on Crane's data obtains $c(f)$ and $d(f)$ for any frequency in the 10 to 95 GHz region.

Variability of attenuation of earth-space links is, as yet, not directly assessable by theoretical formulation. Thus, it is necessary to **input, say,** two additional rain rate distributions corresponding to the lower and upper confidence limits of R_0 in order to evaluate corresponding confidence limits on an attenuation distribution. This, of course, assumes no variance in the many parameters surrounding the attenuation formulation. This is clearly not so, and indicates that the procedure for evaluating attenuation confidence limits is still in need of refinement.

3.3.3 Dutton-Dougherty Computer Model

Dutton has developed an updated computer program (Steele-1979 and Janes, et al - 1978) to predict the annual distribution of tropospheric attenuation due to rain, clouds and atmospheric gases. Entitled DEGP80, the program also computes the phase delay and reflectivity. The required inputs to the program are:

Frequency

Earth station antenna elevation angle

Identification of data stations

Height above surface

Ratio of thunderstorm to non-thunderstorm rain

Time availability

Rainfall rate

Values for average annual atmospheric pressure, humidity, and temperature

The program is valid for frequencies from 1 to 30 GHz and for satellite elevation angles greater than 5 degrees. The program is available from the Institute for Telecommunications Sciences. [See U.S. Dept. of Commerce (1981)].

3.4 THE GLOBAL MODEL

The Global Model has been developed in two forms. Both of these forms utilize cumulative rain rate data to develop cumulative attenuation statistics. The first form, called the Global

Prediction Model (**CCIR-1978a**, Dec. P/105-E, 6 June), employs a path averaging parameter "r" to relate the point rain rate to the average rain rate along the path from the ground station to the point where the hydrometers exist in the form of ice crystals. The later form of the model (Crane and **Blood** - 1979, Crane - 1980a, **1980b**) **includes** path averaging implicitly, and adjusts the isotherm heights for various percentages of time to account for the types of rain structures which dominate the cumulative statistics for the respective percentages of time. Both forms will be described here because the latter is the recommended form for use by system designers, but the earlier form is **computationally** easy to implement and allows rapid computation with a hand-held calculator.

3.4.1 Rain Model

The rain model employed in both forms of the attenuation model is used for the estimation of the annual attenuation distribution to be expected on a specific propagation link. It differs from most other rain models in that it is based entirely on meteorological **observations**, not attenuation measurements. The rain model, combined with the attenuation estimation, was tested by comparison with attenuation measurements. This procedure was used to circumvent the requirement for attenuation observations over a span of many years. The total attenuation model is based upon the use of independent, meteorologically derived estimates for the cumulative distributions of point rainfall rate, horizontal path averaged rainfall rate, the vertical distribution of rain intensity, and a theoretically derived relationship between specific attenuation and rain rate obtained using median observed drop size distributions at a number of rain rates.

The first step in application of the model is the estimation of the instantaneous point rain rate (R_p) distributions. The Global Prediction Model provides median distribution estimates for broad geographical regions; **eight** climate regions A through H are designated to classify regions covering the entire globe.

Figures 3.4-1 and 3.4-2 show the geographic rain climate regions. for the continental and ocean areas of the earth. The United States and European portions are further expanded in Figures 3.4-3 and 3.4-4 respectively.

The climate regions depicted by the Global Model are very broad. The upper and lower rain rate bounds provided by the nearest adjacent region have a ratio of 3.5 at 0.01 percent of the year for the proposed CCIR climate region D, for example, producing an attendant ratio of upper-to-lower bound attenuation values of 4.3 dB at 12 GHz. This uncertainty in the estimated attenuation value can be reduced by using rain rate distributions tailored to a particular area if long term statistics are available. Using the subdivision of climate regions B and D in the continental United States, Canada, and Europe also helps to reduce the uncertainty in the estimates.

The values of R_p may be obtained from the rain rate distribution curves of Figure 3.4-5. Figure 3.4-5a shows the curves for the eight global climate regions designated A through H for one minute averaged surface rain rate as a function the percent of year that rain rate is exceeded. The distributions for the region B and D subregions are shown in Figure 3.4-5b. Note that the distribution for region D_2 corresponds to that for D. Numerical values of R_p are provided in Table 3.4-1 for all regions and subregions.

3.4.2 Description of the Rain Attenuation Region

A path averaged rainfall rate $R = rR_p$, where r is defined as the effective path average factor, is useful for the estimation of attenuation for a line-of-sight radio relay system but, for the estimation of attenuation on a slant path to a satellite, account must be taken of the variation of specific attenuation with height. The atmospheric temperature decreases with height and, above some height, the precipitation particles must all be ice particles. Ice or snow do not produce significant attenuation; only regions with liquid water precipitation particles are of interest in the

Table 3.4-1. Point Rain Rate Distribution Values (mm/hr)
Versus Percent of Year Rain Rate is Exceeded

Percent of Year	RAIN CLIMATE REGION												Minutes per Year	Hours per Year
	A	'1	B	'2	C	'1	D=D ₂	'3	E	F	G	H		
0.001	28.5	45	57.5	70	78	90	108	126	165	66	185	253	5.26	0.09
0.002	21	34	44	54	62	72	89	106	144	51	157	220.5	10.5	0.18
0.005	13.5	22	28.5	35	41	50	64.5	80.5	118	34	20.5	178	26.3	0.44
0.01	10.0	15.5	19.5	23.5	28	35*5	49	63	98	23	94	147	52.6	0.88
0.02	7.0	11.0	13.5	16	18	24	35	48	78	15	72	119	105	1.75
0.05	4.0	6.4	8.0	9.5	11	14.5	22	32	52	8.3	47	86.5	263	4.38
0.1	2.5	4.2	5.2	6.1	7.2	9.8	14.5	22	35	5.2	32	64	526	8.77
0.2	1.5	2.8	3.4	4.0	4.8	6.4	9.5	14.5	21	3.1	11.8	43.5	1052	17.5
0.5	0.7	1.5	1.9	2.3	2.7	3.6	5.2	7.8	10.6	1.4	12.2	22.5	2630	43.8
1.0	0.4	1.0	1.3	1.5	1.8	2.2	3.0	4.7	6.0	0.7	8.0	12.0	5260	87.7
2.0	0.1	0.5	0.7	0.8	1.1	1.2	1.5	1.9	2.9	0.2	5.0	5.2	10520	175
5.0	0.0	0.2	0.3	0.3	0.5	0.0	0.0	0.0	0.5	0.0	1.8	1.2	26298	438

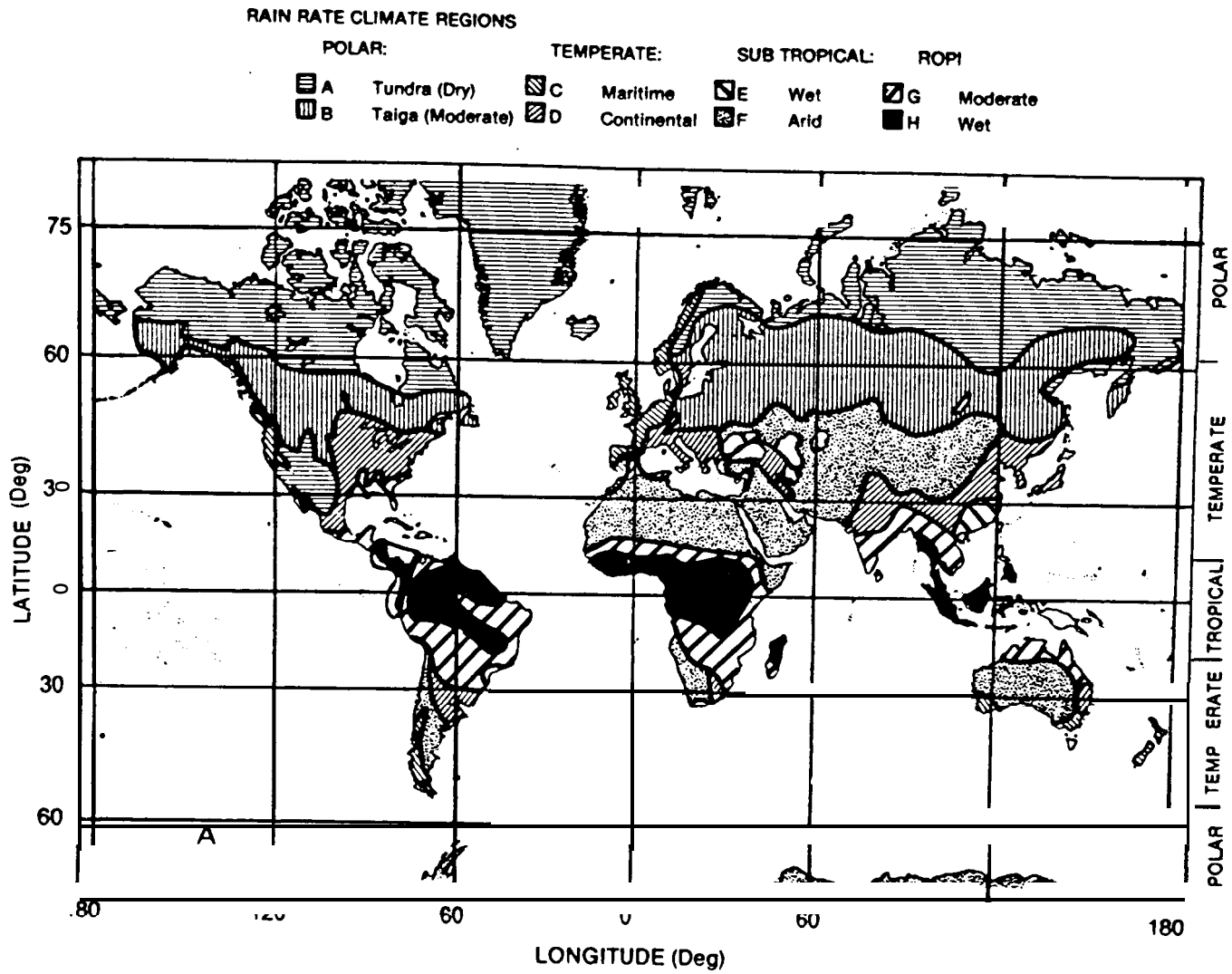


Figure 3.4-1. Global Rain Rate Climate Regions for the Continental Areas

RAIN RATE CLIMATE REGIONS

POLAR:

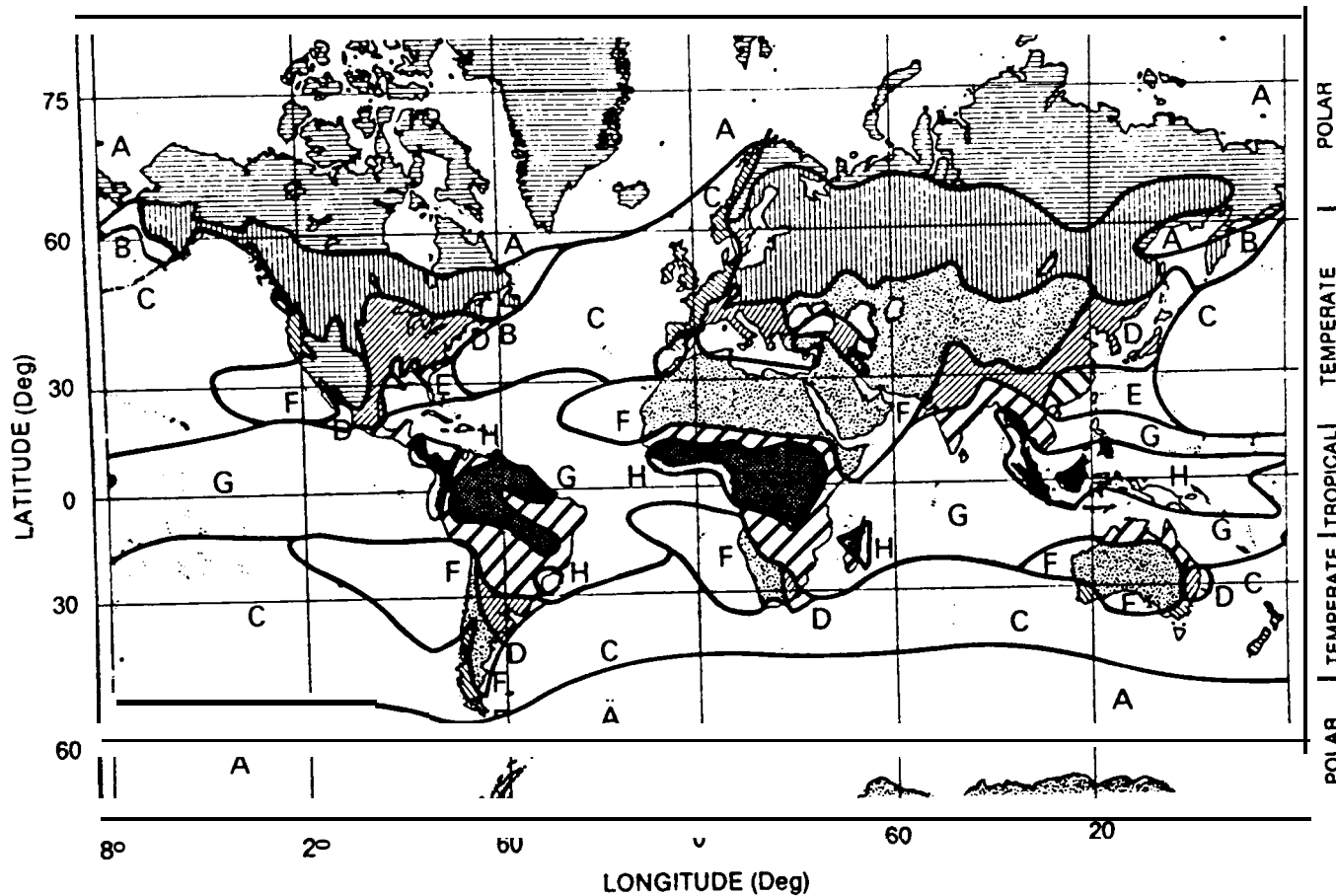
- A Tundra (Dry)
- B Taiga (Moderate)

TEMPERATE:

- C Maritime
- D Continental

SUB TROPICAL:

- E Wet
- F Arid
- G Moderate
- H Wet



3-22

Figure 3.4-2. Global Rain Rate Climate Regions including the Ocean Areas

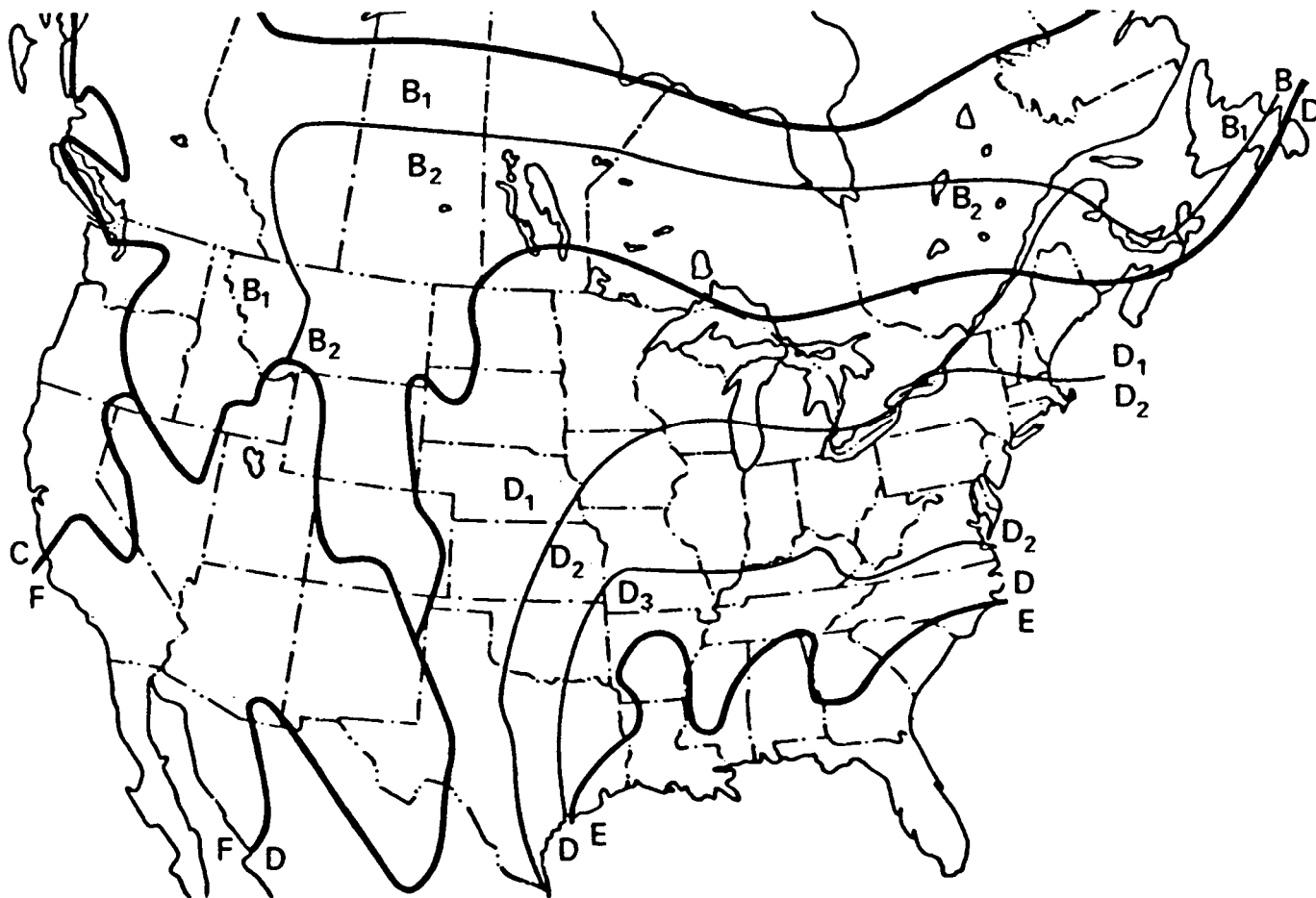


Figure 3.4-3. Rain Rate Climate Regions for the Continental U.S. and Southern Canada

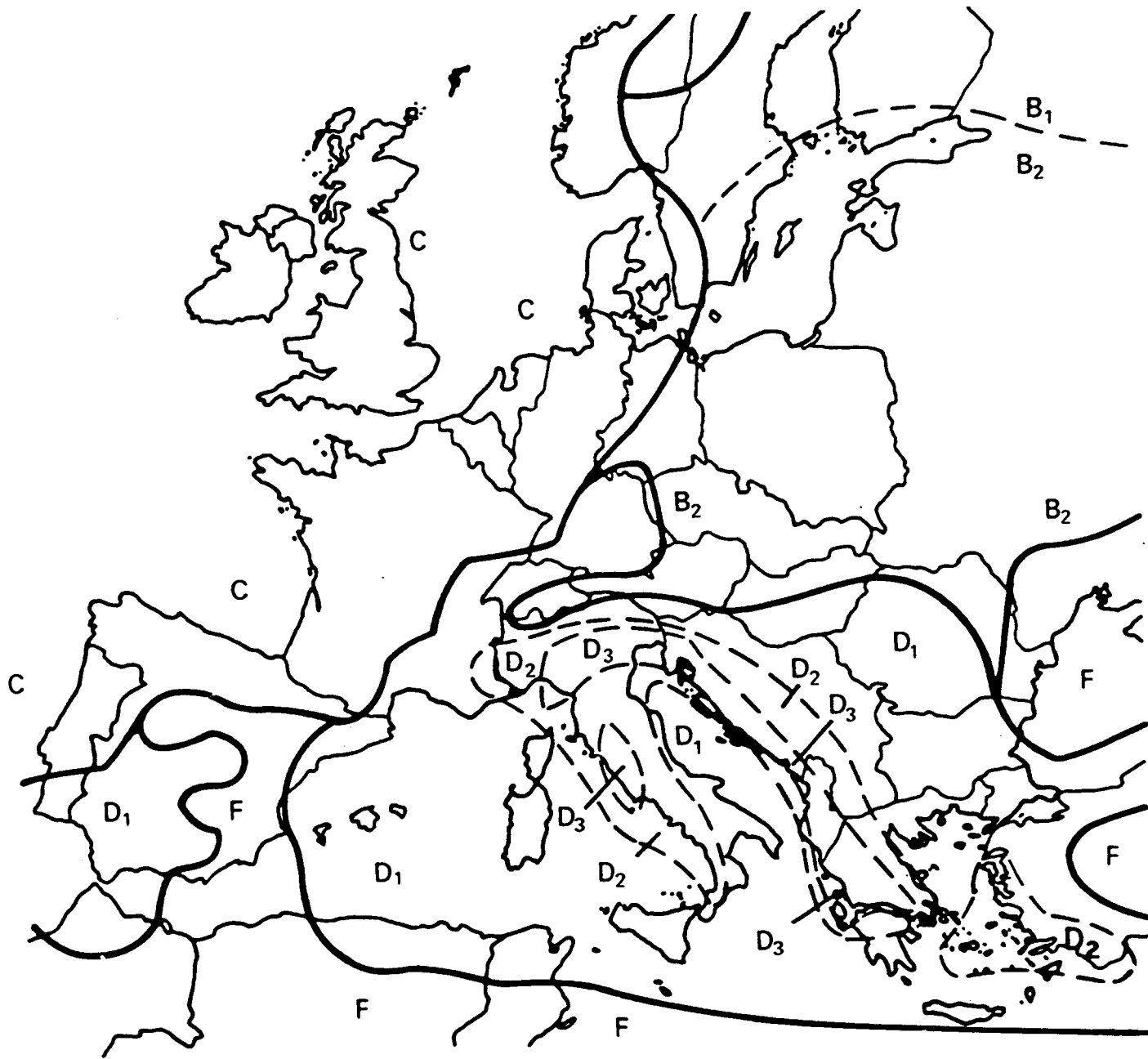


Figure 3.4-4. Rain Rate Climate Regions of Europe

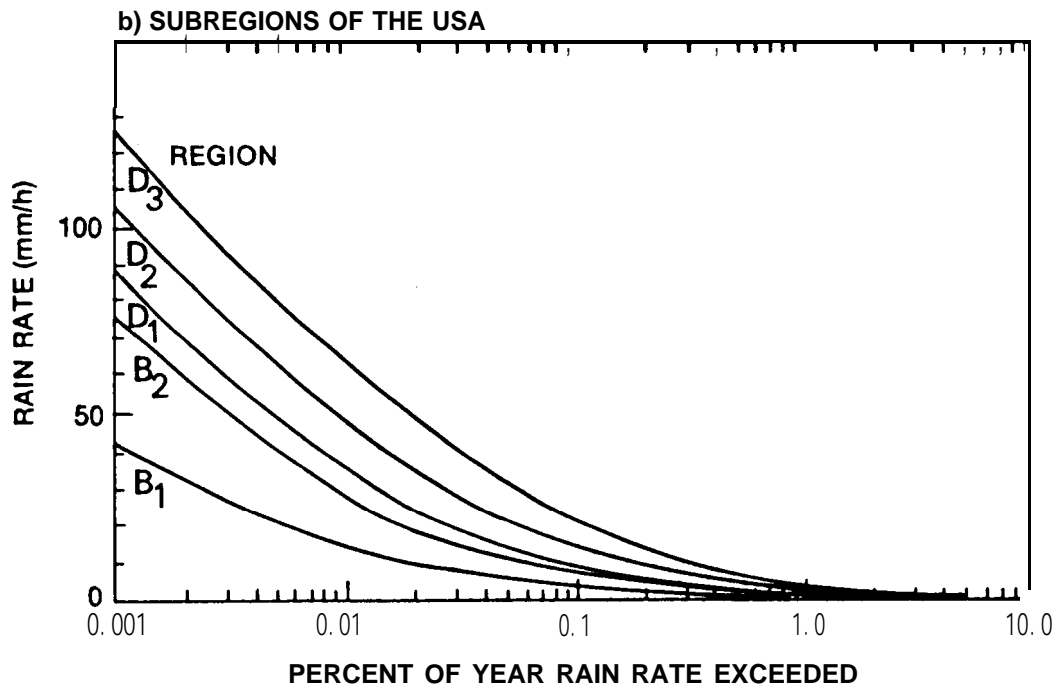
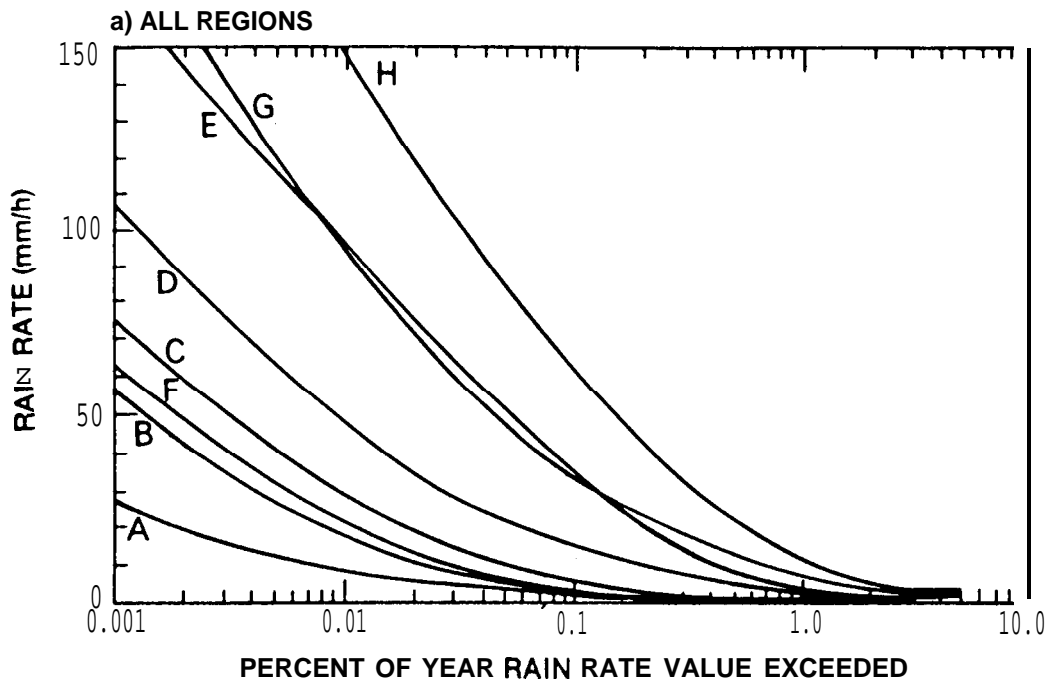
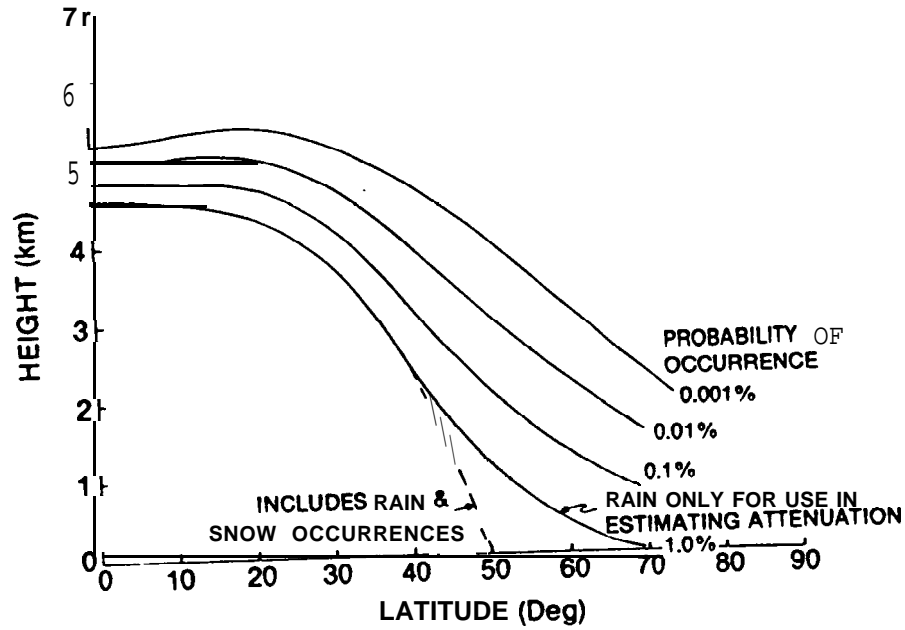


Figure 3.4-5. Point Rain Rate Distributions as a Function of Percent of Year Exceeded

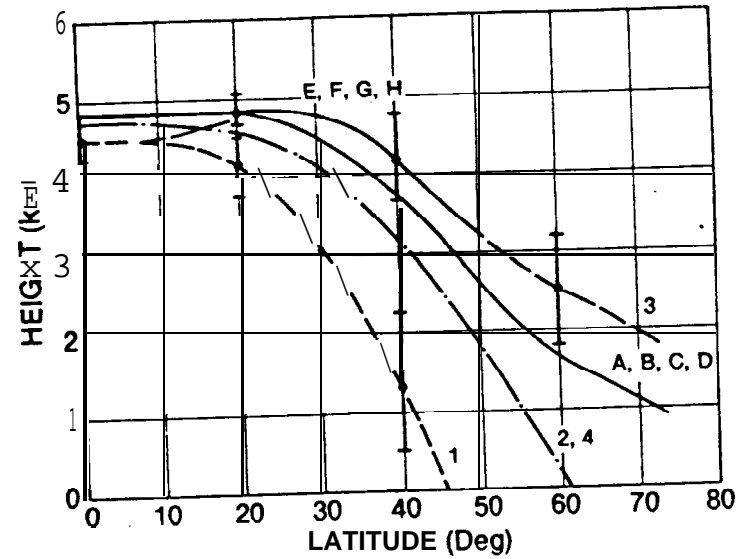
estimation of attenuation. The size and number of rain drops per unit volume may vary with height. Measurements made using weather radars show that the reflectivity of a rain volume may vary with height but, on average, the reflectivity is roughly constant with height to the height of the 0°C isotherm and decreases above that height. The rain rate may be assumed to be constant to the height of the 0°C isotherm at low rates and this height may be used to define the upper boundary of the attenuating region. A high correlation between the 0°C height and the height to which liquid rain drops exist in the atmosphere should not be expected for the higher rain rates because large liquid water droplets are carried aloft above the 0° height in the strong updraft cores of intense rain cells. It is necessary to estimate the rain layer height appropriate to the path in question before proceeding to the total attenuation computation since even the 0°C isotherm height depends on latitude and general rain conditions.

As a model for the prediction of attenuation, the average height of the 0° isotherm for days with rain was taken to correspond to the height to be expected one percent of the year. The highest height observed with rain was taken to correspond to the value to be expected 0.001 percent of the year, the average summer height of the -5°C isotherm. The latitude dependence of the heights to be expected for surface point rain rates exceeded one percent of the year and 0.001 percent of the year were obtained from the latitude dependence provided by Oort and Rasmussen (1971). The resultant curves are presented in Figure 3.4-6. For the estimation of model uncertainty, the seasonal rms uncertainty in the 0°C isotherm height was 500 m or roughly 13 percent of the average estimated height. The value of 13 percent is used to estimate the expected uncertainties to be associated with Figure 3.4-6.

The correspondence between the 0°C isotherm height values and the excessive precipitation events showed a tendency toward a linear relationship between R_p and the 0°C isotherm height H_0 for high values of R_p . Since at high rain rates, the rain rate distribution



a) Variable Isotherm



- MODEL FOR RAIN RATE CLIMATES A THROUGH H
- - - ANNUAL
- - - SEASONAL 1 — WINTER (NORTHERN HEMISPHERE)
- 2 — SPRING
- 3 — SUMMER
- 4 — FALL

b) 0°C Isotherm Height

Figure 3.4-6. Effective Heights for Computing Path Lengths Through Rain Events

function displays a nearly linear relationship between R_p and $\log P$ (P is probability of occurrence), the interpolation model used for the estimation of H_0 for P between 0.001 and one percent is assumed to have the form, $H_0 = a + b \log p$. The relationship was used to provide the intermediate values displayed in Figure 3.4-6a. In Figure 3.4-6b are shown the 0°C isotherms for various latitudes and seasons.

3.4.3 Attenuation Model

The complete model for the estimation of attenuation on an earth-space path starts with the determination of the vertical distance between the height of the earth station and the 0°C isotherm height ($H_0 - H_g$ where H_g is the ground station height) for the percentage of the year (or R_p) of interest. The path horizontal projection distance (D) can then be obtained by:

$$D = \begin{cases} (H_0 - H_g)/\tan \theta & \theta \geq 10^\circ \\ E\psi (\psi \text{ in radians}) & \theta < 10^\circ \end{cases} \quad (3.4-1)$$

where

H_0 = height of 0°C isotherm

H_g = height of ground terminal

θ = path elevation angle

and

$$\psi = \sin^{-1} \left\{ \frac{\cos \theta}{H_0 + E} \left[(H_g + E)^2 \sin^2 \theta + 2E(H_0 - H_g) + H_0^2 - H_g^2 \right]^{1/2} - (H_g + E) \sin \theta \right\} \quad (3.4-2)$$

$$= \cos^{-1} \left[\frac{\cos \theta}{H_0 + E} (E + H_g) \right] - e$$

where

E = effective earth's radius (8500 km).

The specific attenuation may be calculated for an ensemble of rain drops if their size and shape number densities are known. Experience has shown that adequate results may be obtained if the Laws and Parsons (1943) number density model is used for the attenuation calculations (Crane-1966) and a power law relationship is fit to calculated values to express the dependence of specific attenuation on rain rate (Olsen et al-1978). The parameters a and b of the power law relationship:

$$a = aR_p^b \quad (3.4-3)$$

where a = specific attenuation (dB/km)

R_p = point rain rate (mm/hour)

are both a function of operating frequency. Figures 3.4-7 and 3.4-8 give the **-multiplier, a(f)** and exponent **b(f)**, respectively at frequencies from 1 to 100 GHz. The appropriate a and b parameters may also be obtained from Table 3.4-2 and used in computing the total attenuation from the model. Alternately, values of a and b from Tables 2.3-2 or 2.3-3 may be used.

3.4.3.1 Path Averaged Rain Rate Technique. The path averaged rain rate exceeded for a specified percentage of the time may differ significantly from the surface point rain rate exceeded for the same percentage of the time. The estimation of the path averaged values from the surface point values requires detailed information about the spatial correlation function for rain rate. Adequate spatial data are not currently available. A sufficient number of observations using rain gauge networks are available to provide a basis for a point to path average model. Observations for 5 and 10 km paths are presented in Figures 3.4-9 and **3.4-10**, respectively. The effective path average **factor, r**, represents the relationship between point and path averaged rain rate as

$$R_{\text{path}} = r \cdot R_p \quad (3.4-4)$$

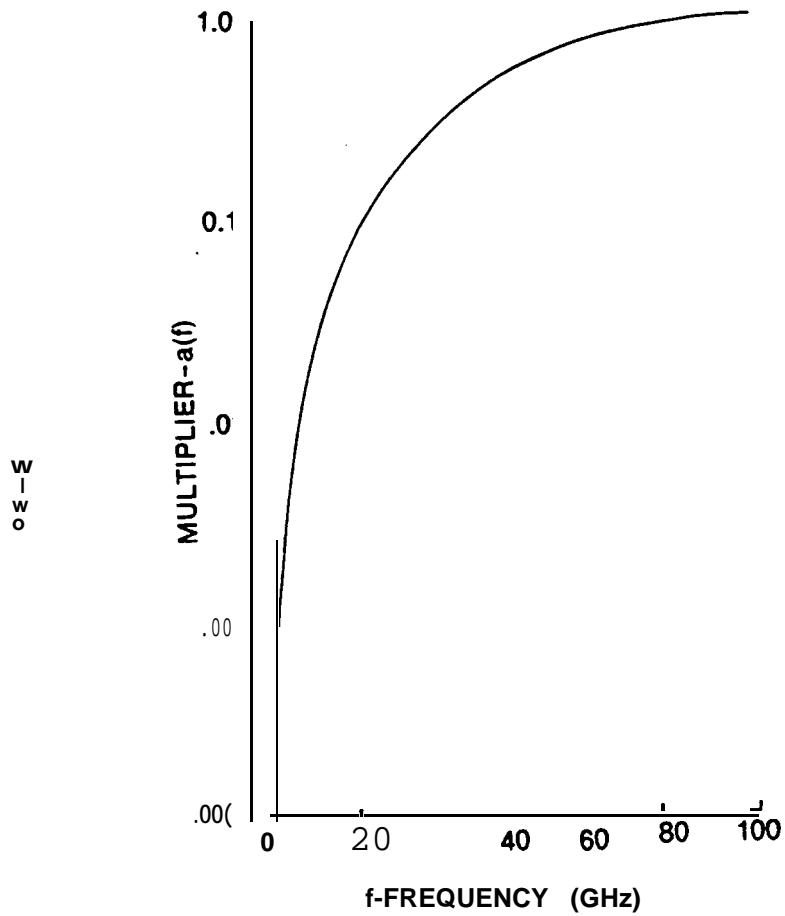


Figure 3*4-7* Multiplier Coefficient in the Specific Attenuation Relation

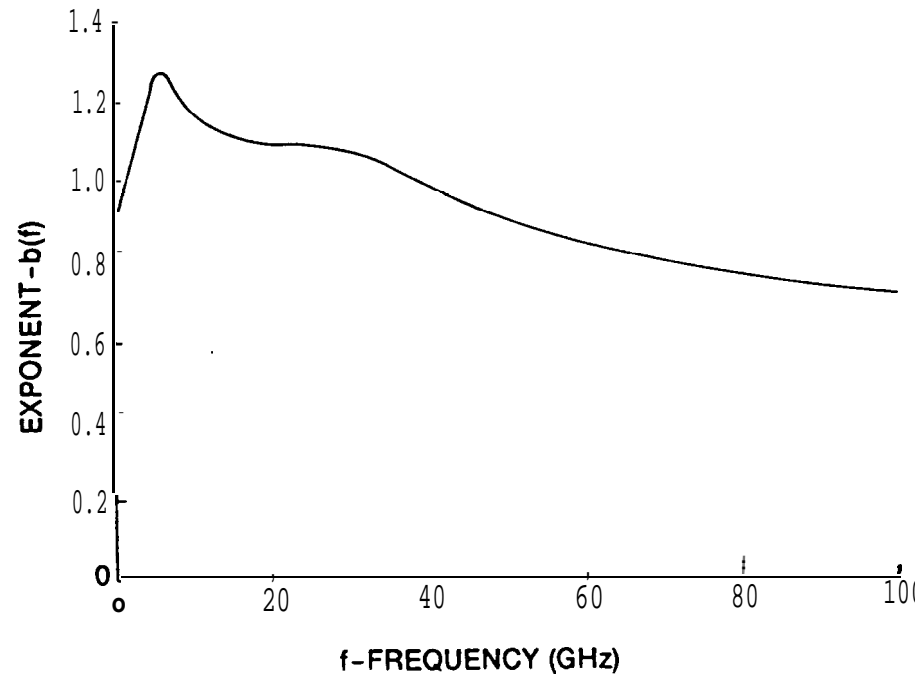


Figure 3.4-8. Exponent Coefficient in the Specific Attenuation Relation

Table 3.4-2. Parameters for Computing Specific Attenuation:
 $= aR^b, 0^\circ\text{C}$, Laws and Parson Distribution
 (Crane-1966)

Frequency f - GHz	Multiplier a(f)	Exponent b(f)
1	0.00015	0.95
4	0.00080	1.17
5	0.00138	1.24
6	0.00250	1.28
7.5	0.00482	1.25
10	0.0125	1.18
12.5	0.0228	1.145
15	0.0357	1.12
17.5	0.0524	1.105
20	0.0699	1.10
25	0.113	1.009
30	0.170	1.075
35	0.242	1.04
40	0.325	0.99
50	0.485	0.90
60	0.650	0.84
70	0.780	0.79
80	0.875	0.753
90	0.935	0.730
100	0.965	0.715

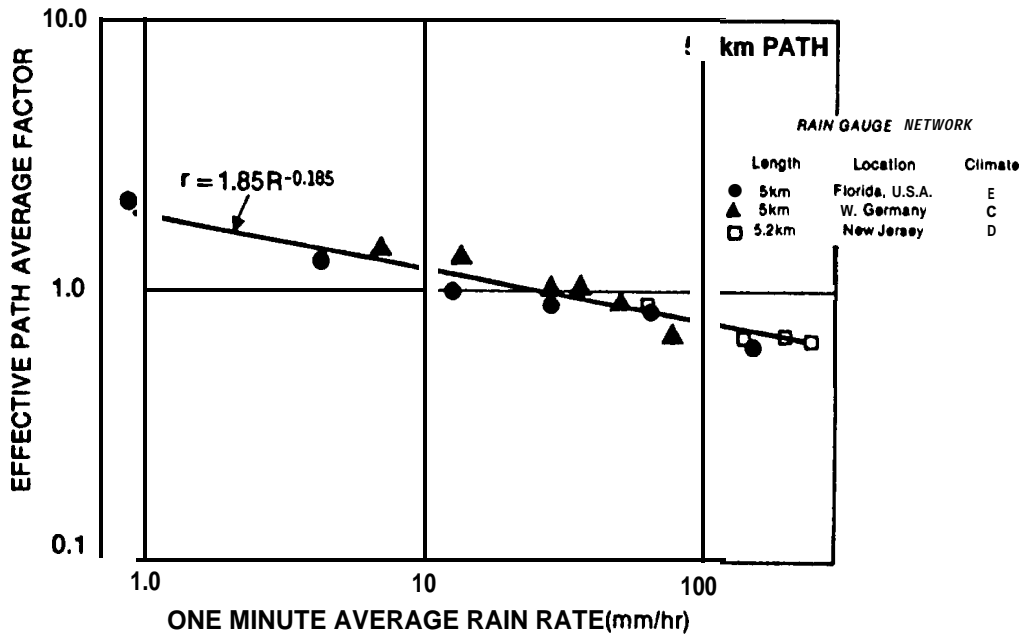


Figure 3.4-9. Effective Path Average Factor Versus Rain Rate, 5 km Path

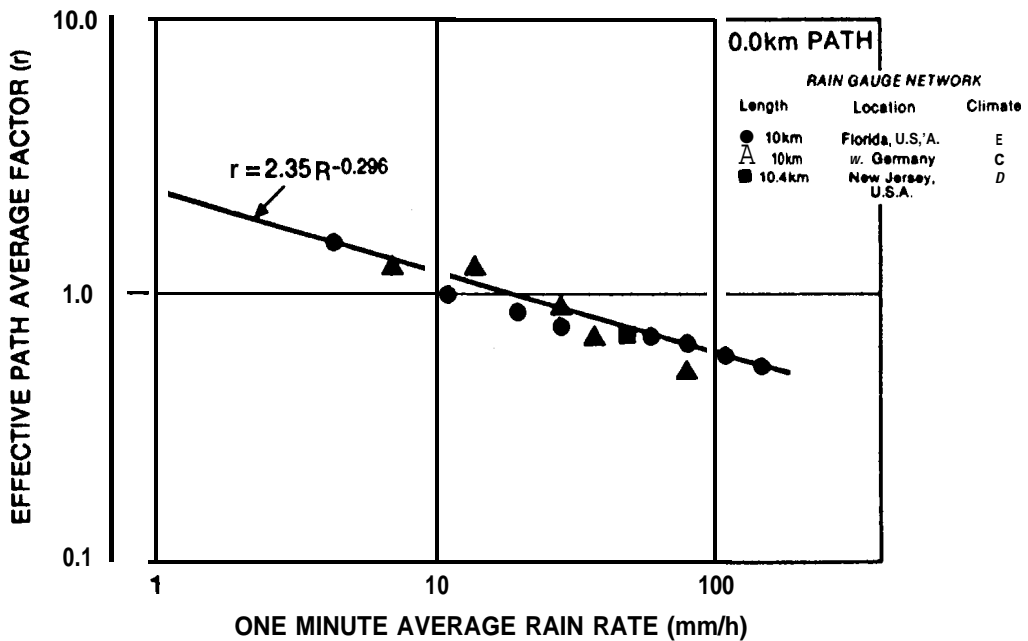


Figure 3.4-10. Effective Path Average Factor Versus Rain Rate, 10 km Path

where R_{path} and R_p are the path and point rainfall rates at the same probability of occurrence.

Figure 3.4-11 represents the construction of an effective path average factor using data from paths between 10 and 22.5 km in length. The values of r were obtained by **assuming** that the occurrence of rain with rates in excess of 25 mm/hour were independent over distances larger than 10 km. The estimation of path averaged rain rate then depends upon modeling the **change** in occurrence probability for a fixed path average value, not the change in path average value for a fixed probability. Using D_0 as the reference path length ($D_0 = 22.5$ km for Figure 3.4-11), the exceedance probabilities for the path averaged values were multiplied by D_0/D where D was the observation path length to estimate the path average factor for a path of length D_0 .

The path attenuation caused by rain is approximately determined from the path averaged rain rate by

$$A \approx L r a R_p^b \quad (3.4-5)$$

where A is path attenuation, L is the length of the propagation path or D_0 , whichever is shorter, r is the effective path average factor, R is the point rainfall rate exceeded P percent of the time, and a and b are coefficients used to estimate specific attenuation for a given rain rate. Using this model and propagation paths longer than 22.5 km, the effective path average factor for 22.5 km path may be calculated from simultaneous point rain rate distribution and attenuation distribution data. Results for a number of paths in rain rate climates C and D are presented in Figure 3.4-12. The line plotted on this figure is the power law relationship fit to all the data displayed in Figure 3.4-11. The observations at 13 and 15 GHz are in excellent agreement with the model based solely on rain gauge network data. At lower frequencies, the discrepancy is larger, being as much as a factor of 2. At 11 GHz, the model appears to underestimate the observed attenuation by a factor of 2. It is

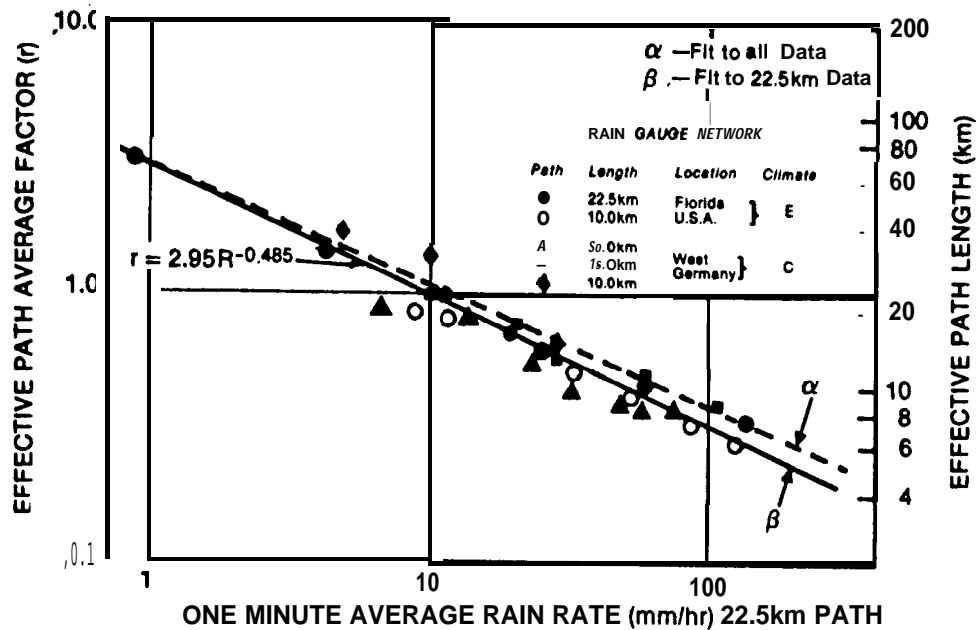


Figure 3.4-11. Effective Path Average Factor Versus Rain Rate

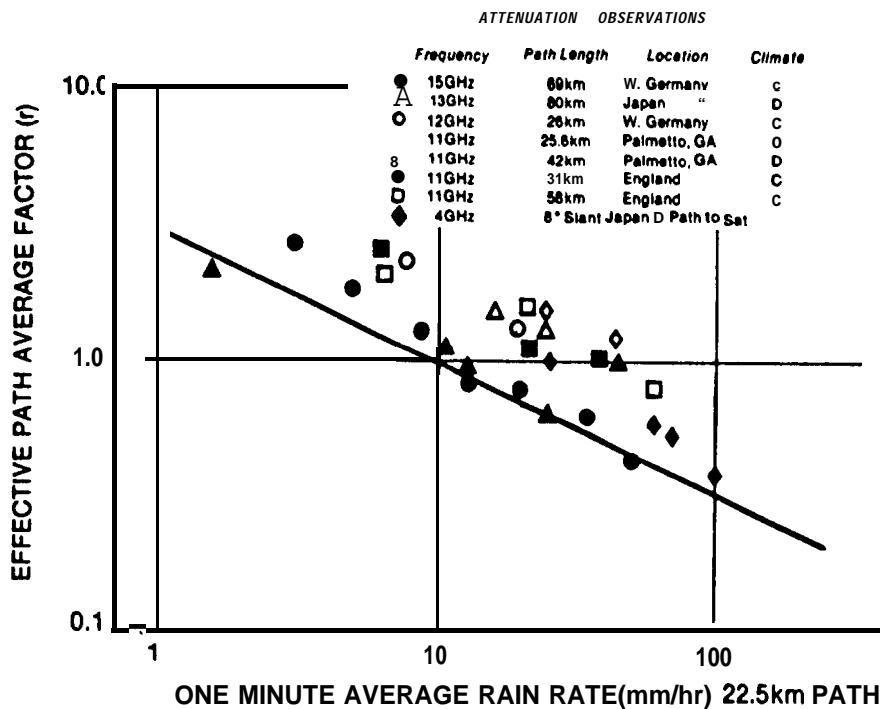


Figure 3.4-12. Effective Path Average Factor Versus Rain Rate Derived from Attenuation Measurements

noted that simultaneous point rain rate observations were used in the construction of Figure 3.4-12, not the rain rate distributions for each climate region. Since fades due to **multipath** must be removed from the analysis prior to making the comparison in Figure 3.4-12 and **multipath** effects tend to be relatively more important at frequencies below 13 GHz, the lack of agreement displayed in Figure 3.4-12 may be due to effects other than rain.

A power law approximation to the effective path average factors depicted in Figures 3.4-9 through 3.4-11 may be used to model the behavior of the effective path average factor for paths shorter than 22.5 km. Letting the effective path average factors be expressed by

$$r \approx \gamma (D) R_p^{-\delta(D)} \quad (3.4-6)$$

where D is the surface projection of the propagation path and the model curves for $\gamma(D)$ and $\delta(D)$ are given in Figure 3.4-13 and 3.4-14. Figure 3.4-15 displays the dependence of the modeled effective path average factor on point rain rate.

Attenuation prediction for Earth-space paths requires the estimation of rain rate along a slant path. Statistical models for rain scatter indicate that the reflectivity, hence, specific attenuation or rain rate, is constant from the surface to the height of the 00C isotherm (**Goldhirsh** and Katz 1979). By assuming that the specific attenuation is statistically independent of height for altitudes below the 0°C isotherm the path averaged rain rate (or specific attenuation) can be estimated using the model in Figures 3.4-13 and 3.4-14. For application, the surface projection of the slant path below the melting layer is used to define the surface path length, D. The attenuation on an Earth-space path for an elevation angle higher than 10° is given by:

$$A = \frac{H}{\sin \theta} a(f) \gamma(D) R_p^{b(f)-d(D)} \quad (3.4-7)$$

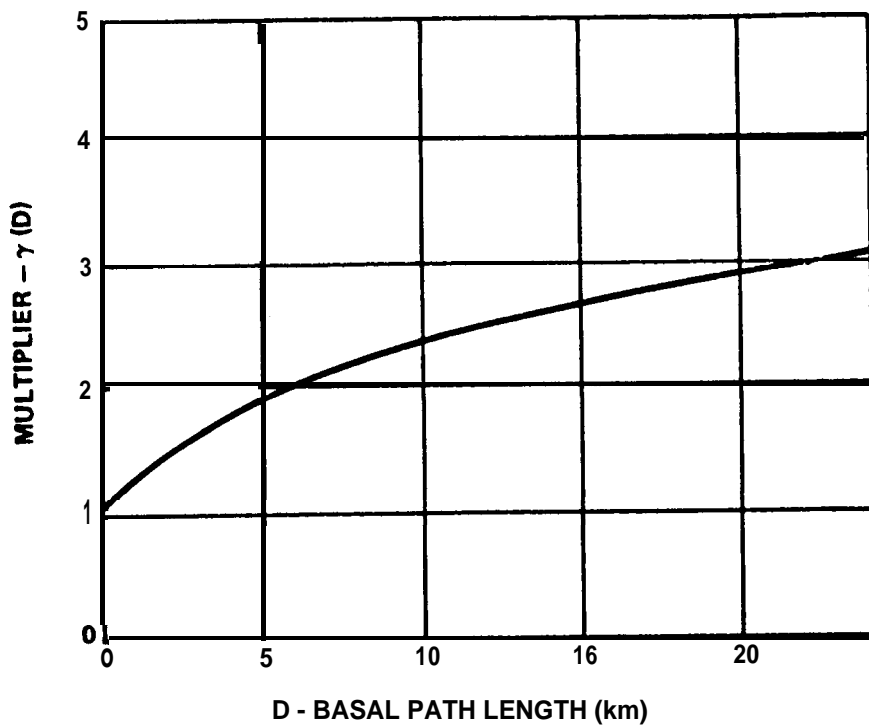


Figure 3.4-13. Multiplier in the Path Averaging Model

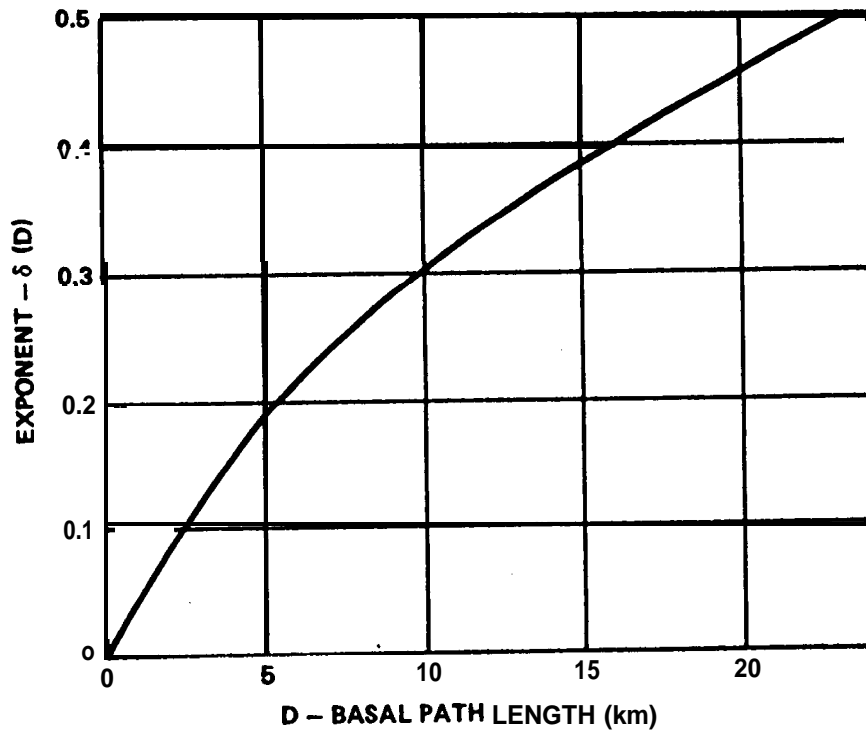


Figure 3.4-14. Exponent in the Path Averaging Model

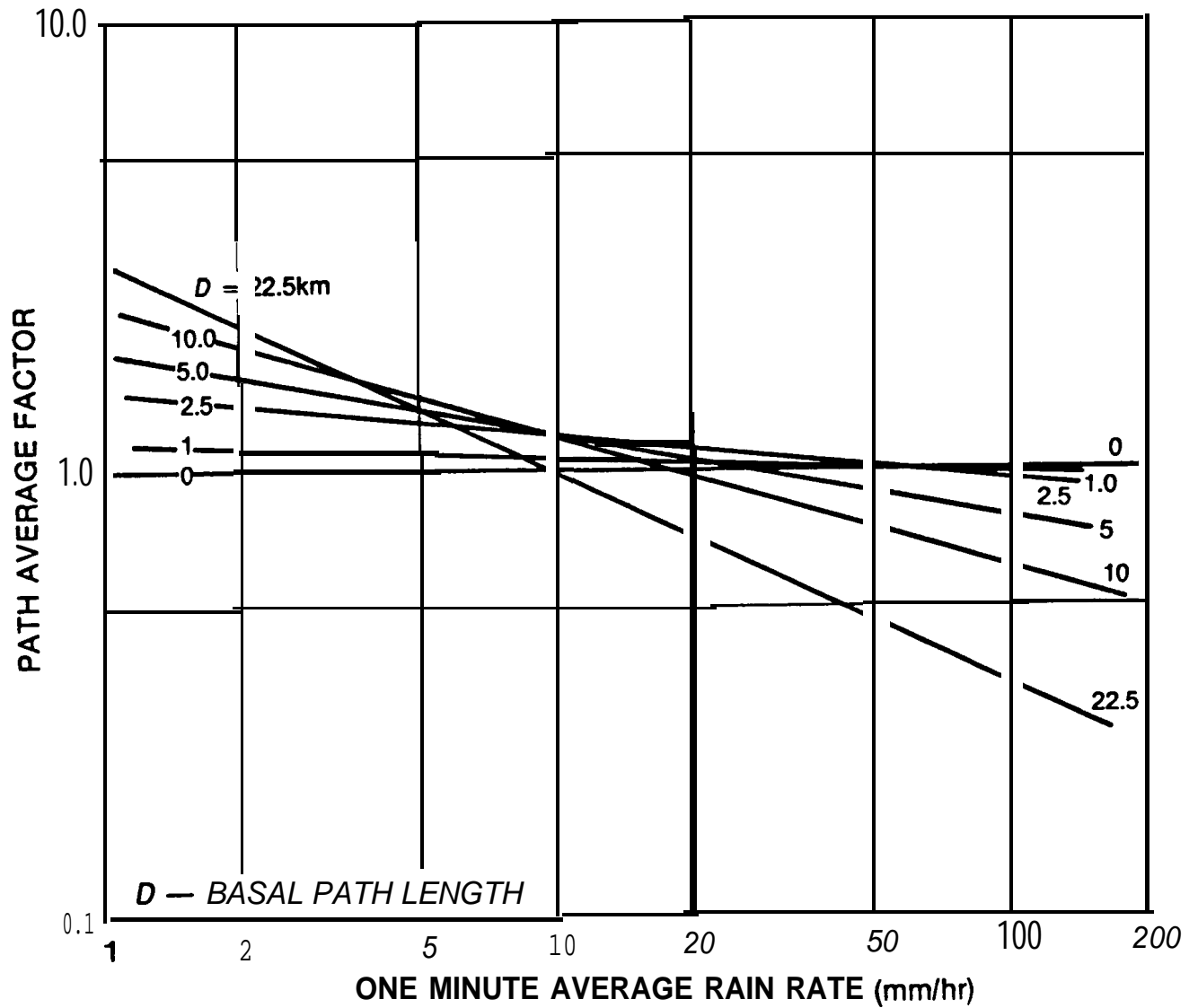


Figure 3.4-15. Effective Path Average Factor Model for Different Basal Path Lengths

where H is the height of the 0°C isotherm (see Figure 3.4-6b), θ is the elevation angle ($\theta > 10^\circ$) and $D = H/\tan \theta$. For application at elevation angles lower than 10° , the effect of refraction by the troposphere and of the earth's curvature should be taken into account in the calculation of D. If D exceeds 22.5 km, a D_o of 22.5 km is used for the calculation of the effective path average factor and the occurrence probabilities are multiplied by D/D_o .

3.4.3.2 Variable Isotherm Height Technique. The variable isotherm height technique uses the fact that the effective height of the attenuating medium changes depending on the type of rainfall event. Also, various types of rainfall events selectively influence various percentages of time throughout the annual rainfall cycle. Therefore, a relation exists between the effective isotherm height and the percentage of time that the rain event occurs. This relation has been shown earlier in Figure 3.4-6a. Again the total attenuation is obtained by integrating the specific attenuation along the path. The resulting equation to be used for the estimation of slant path attenuation is:

$$A = \frac{a R_p^b}{\cos \theta} \left[\frac{e^{UZb}-1}{Ub} - \frac{X^{be}YZb}{Yb} + \frac{X^{be}YDb}{Yb} \right]; \theta \geq 10^\circ \quad (3.4-8)$$

where U, X, Y and Z are empirical constants that depend on the point rain rate. These constants are:

$$u = \frac{1}{Z} [\ln(Xe^{YZ})] \quad (3.4-9)$$

$$x = 2.3 R_p^{-0.17} \quad (3.4-10)$$

$$Y = 0.026 - 0.03 \ln R_p \quad (3.4-11)$$

$$z = 3.8 - 0.6 \ln R_p \quad (3.4-12)$$

for lower elevation angles $\theta < 10^\circ$

$$A = \frac{L}{D} a R_p^b \left[\frac{e^{UZb-1}}{Ub} - \frac{X^{be}YZb}{Yb} + \frac{X^{be}YDb}{Yb} \right] \quad (3.4-13)$$

where

$$L = [(E + H_g)^2 + (E + H_o)^2 - 2(E + H_g)(E + H_o) \cos \psi]^{\frac{1}{2}} \quad (3.4-14)$$

$$= [(E + H_g)^2 \sin^2 \theta + 2E(H_o - H_g) + H_o^2 - H_g^2]^{\frac{1}{2}} - (E + H_g) \sin \theta$$

ψ = path central angle defined above.

3-4.4 Application of the Global Model

Section 6.3.2.1 gives a step-by-step procedure for applying the Global Model, using the variable isotherm technique. Schwab (1980) applied this model on a worldwide basis to find downlink availability for specified margin and frequency. An example of the results of his work is shown in Figure 3.4-16. It is interesting to compare this figure with the rain climate region map of Figure 3.4-2.

3.5 THE TWO-COMPONENT MODEL

The Two-Component (T-C) rain attenuation model (Crane-1982) determines the probability of exceeding a given attenuation threshold. The Model's name relates to the fact that two distinctive types of rain events are addressed: convective cell and widespread "debris." The characterization of climatic zones is identical to the Global Model in terms of rain rates. The T-C Model was formulated in such a way that it might later be extended to site diversity systems, rain scatter interference, and attenuation duration statistics.

The fundamental approach in the T-C Model is to determine the probabilities for exceeding a given attenuation with convective rain and debris separately. The sum of these probabilities is then taken as the total probability of exceeding the given rain attenuation threshold.

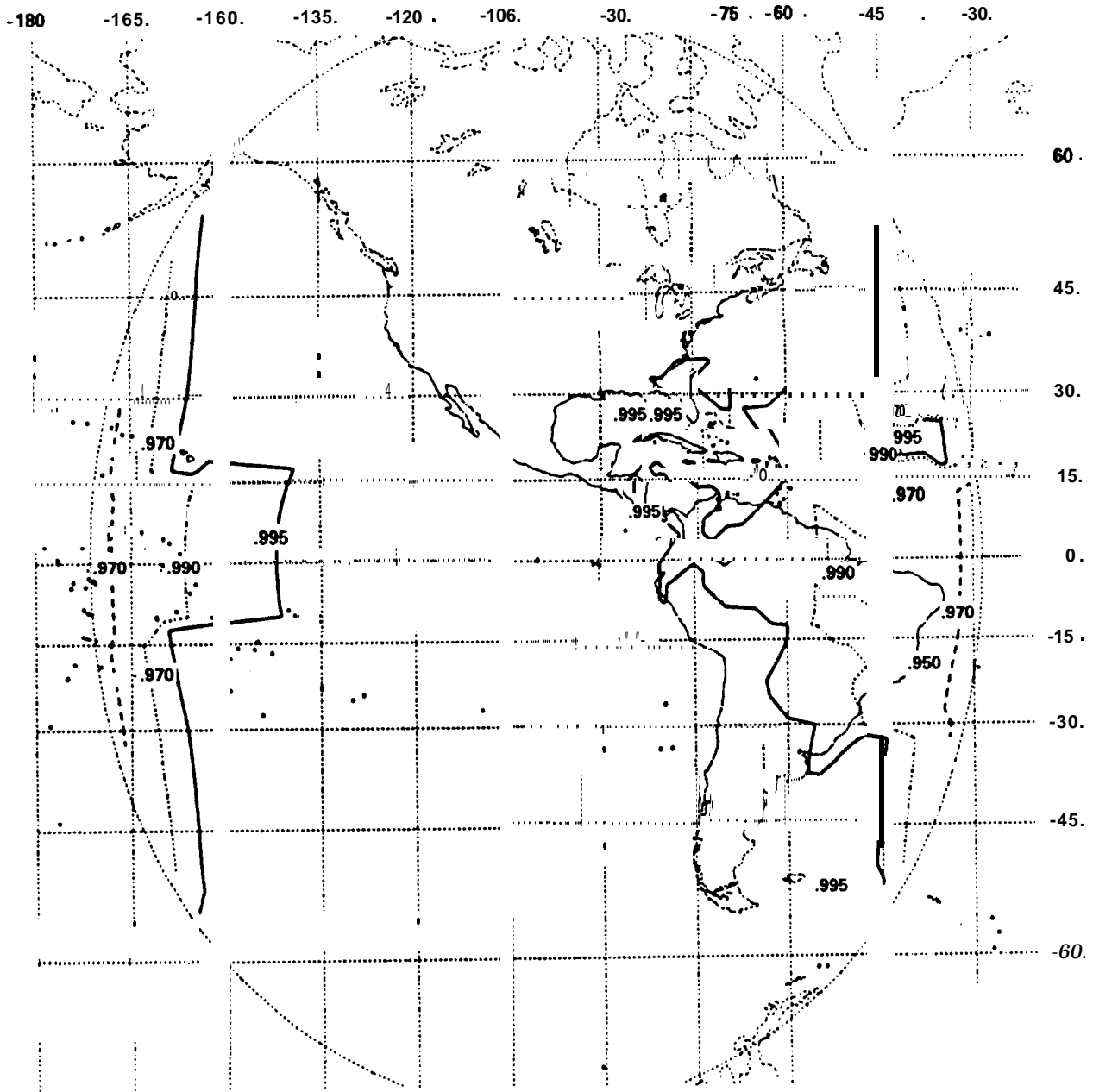


Figure 3.4-16. Availability Contours for Satellite at 100°W With 6 dB Margin Operating at 20 GHz

The projected (horizontal) path lengths for both types of rain are first determined geometrically from 0°C isotherm heights. These heights were modeled from observations during precipitation events using radiosonde data, rain occurrence data and **excessive-precipitation** data for seven spatially separated sites in the US (**Crane-1980a**). The data were extrapolated **globally** using averaged temperature profiles, where only summertime data was used at latitudes higher than 50°. The resulting height versus latitude variations, which do not employ the correlation between rain rate and rain rate height assumed in other models (**e.g., Global**), are:

$$H_c = 3.1 - 1.7 \sin [2(A-45)] \quad (3.5-1)$$

$$H_d = 2.8 - 1.9 \sin [2(A-45)] \quad (3.5-2)$$

where H_c , H_d are the rain heights in kilometers for volume cell (convective) and debris rain types, respectively, and A is the latitude (deg.). The corresponding projected path lengths are then determined geometrically as:

$$D_c, D_d = \frac{(H_{c,d} - H_0) [2 - 2(H_{c,d} - H_0)/8500]}{\tan \theta \sqrt{\tan^2 \theta + (H_{c,d} - H_0)/8500}} \quad (3.5-3)$$

where θ is the slant path elevation angle and H_0 is height of the earth station above sea level (km).

The attenuation along the projected path is determined geometrically from the given slant path attenuation threshold and path elevation angle. This is then used to determine the corresponding rain rates, for volume cell and debris rain **types**, which would produce that amount of attenuation. The two rain types are addressed separately below.

3.5.1 Volume Cell Rain Rate

The average length of a line through a (circular) volume cell (WC) is assumed to be about 2.2 km, based on the average volume cell

area data from a three year radar measurement program conducted in **Goodland, Kansas**. Thus, the effective projected path length through rain (L_c) must be taken to be the lesser of 2.2 km and D_c . If L_c is not determined from D_c ($D_c > W_c$), an adjustment factor (C) is required. In this case, the projected path D_c is longer than the average volume cell width and the integrated path rain rate must embody the effect of debris that is close to the cell. This is modeled as:

$$C = \frac{1 + 0.7 (D_c - W_c)}{1 + (D_c - W_c)}; (D_c - 2.2) > 0 \quad (3.5-4)$$

$$C = 1 \quad ; (D_c - 2.2) \leq 0 \quad (3.5-5)$$

The effective point rain rate (R') for volume cell rain can then be readily determined as:

$$R' = \left(\frac{CA}{KL_c} \right)^{1/\alpha} \quad (3.5-6)$$

where A is the attenuation along the projected path and k and α are the common specific attenuation coefficients for point rainfall rates ($y = KR^\alpha$).

3.5.2 Debris Rain Rate

In debris rain, the rain extent can readily exceed the slant path projection distance. The rain extent (W_d) is, however, dependent on rain rate. The Kansas radar observations indicated a relationship between average rain rate in debris and W_d :

$$W_d = 29.7R^{-0.34}$$

where W_d is the length scale (km) and R is the rain rate (mm/h) for debris. This is more conveniently expressed in terms of attenuation for determining the effective rain rate (R'') in debris. :

$$W_d = 29.71d(a^{-.34}) K^{[.34/(a^{-.34})]} A^{-[.34/(a^{-.34})]} \quad (3.5-7)$$

$$W'_d = \text{minimum}(W_d, D_d) \quad (3.5-8)$$

$$R'' = \left(\frac{A}{kW'_d} \right)^{1/a} \quad (3.5-9)$$

where R'' is the effective rain rate for debris.

3.5.3 Probability of Exceeding an Attenuation Threshold

A simple approximation to the observed (Kansas) rain rate distribution produced by volume cells is an exponential distribution. The debris distribution function was nearly log-normal. The sum of these independent distributions was found to closely fit the empirical rain rate distributions for all climate regions. Thus :

$$P(r \geq R) = P_c(r \geq R) + P_d(r \geq R) \quad (3.5-10)$$

$$= p_c(1 + D_c/W_c) \exp(-R'/R_c)$$

$$+ p_d(1 + D_d/W_d) \eta[(1/\sigma_d)[\ln R'' - \ln R_d]] \quad (3.5-11)$$

where $P(r \geq R)$ is the probability of the observed rain rate r exceeding the specified rain rate R ; $P_{c,d}(r \geq R)$ are the distribution functions for volume cells and debris, respectively; $p_{c,d}$ are the probabilities of a cell and debris, respectively; $R_{c,d}$ are the average rain rates in cells and debris, respectively; σ_d is the standard deviation of the logarithm of the rain rate; and η is the normal distribution function. Values for the parameters p_c , p_d , R_c , and σ_d have been tabulated for each of the Global Model rain climate regions (Crane-1982).

3.6 THE CCIR MODEL

The International Radio Consultative Committee, **CCIR**, adopted a procedure for the prediction of attenuation caused by rain at its XVth Plenary Assembly in Geneva in February 1982 (**CCIR-1982a**). This result was preceded by several years of intense deliberations by representatives of CCIR Study Group V from several nations. The procedure provided the basis for rain attenuation calculations required for international planning and coordination meetings, and Regional and World Administrative Radio Conferences.

The original CCIR procedure has undergone several modifications, including deliberations for the 1982 Conference Preparatory Meeting for **RARC-83** for the Broadcasting Satellite Service (**CCIR-1982b**, **CCIR-1982c**), and the Study Group 5 Inputs for the XVIth Plenary Assembly, in Dubrovnik, Yugoslavia (**CCIR-1985a**, **CCIR-1985b**). The rain characterization and attenuation prediction procedures described in this handbook are the latest published versions, as provided in Reports 563-3 (**CCIR-1986a**), and 564-3 (**CCIR-1986b**), respectively, from the **XVIth** Plenary Assembly. Readers interested in tracing the evolution of the CCIR prediction **procedure** development process are referred to the earlier documents referenced above.

3.6.1 CCIR Rain Characterization

The first element of the CCIR Model involves a global map of fourteen rain climatic zones with associated rainfall intensity cumulative distributions for each region specified (**CCIR-1986a**). Average annual rain rates are given for exceedance times from 0.001 to 1.0 percent. Figure 3.6-1 presents the global map of the CCIR rain climatic zones, ranging from A (light rains) to P (heavy rains). A more detailed map of the **CCIR** climatic zones for the continental United States and Canada is shown in Figure 3.6-2 (**Ippolito**, 1986). Table 3.6-1 lists the rain rate distributions for the fourteen rain climatic zones.

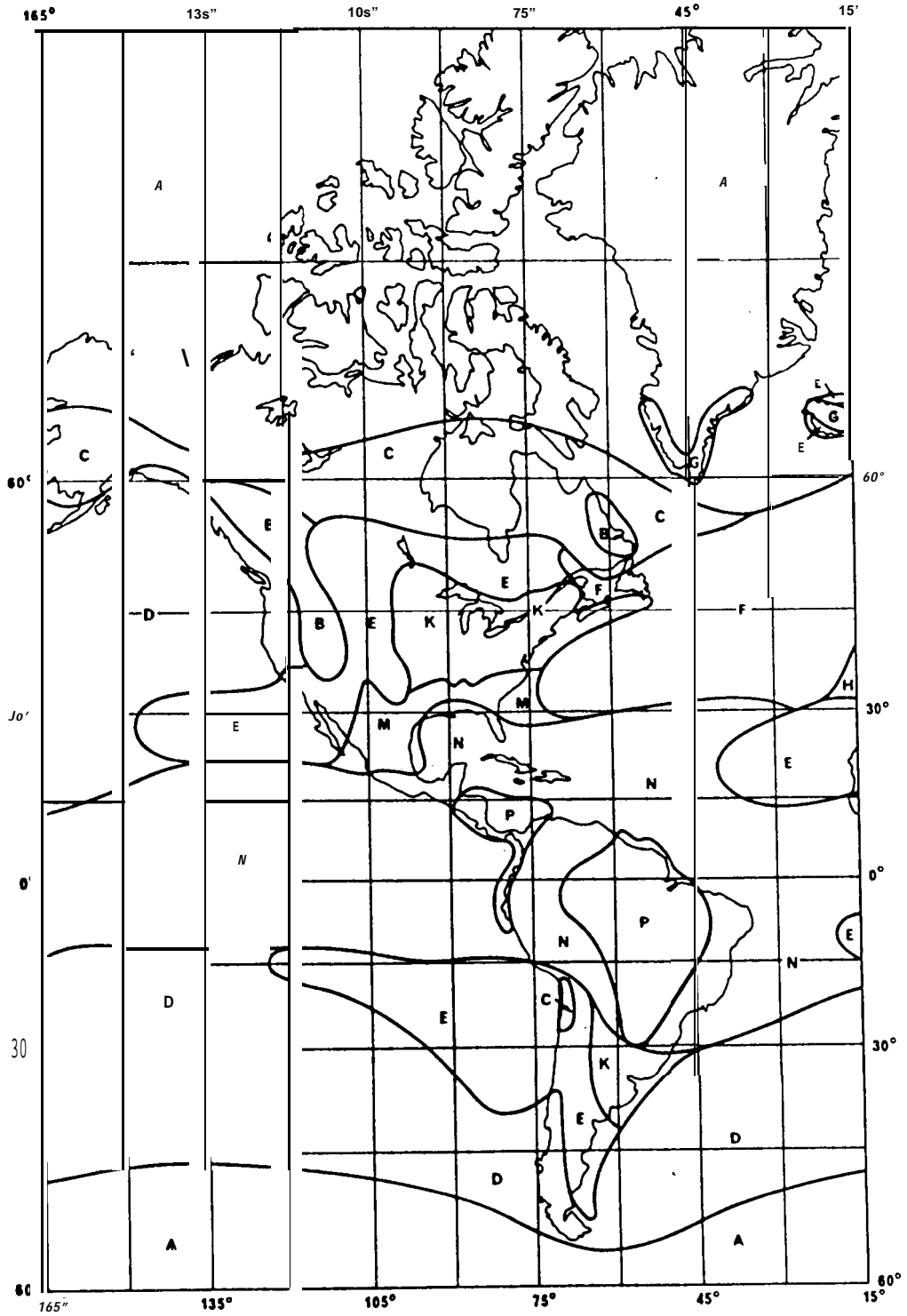


Figure 3.6-1. CCIR Rain Climate Zones (Sheet 1 of 3)

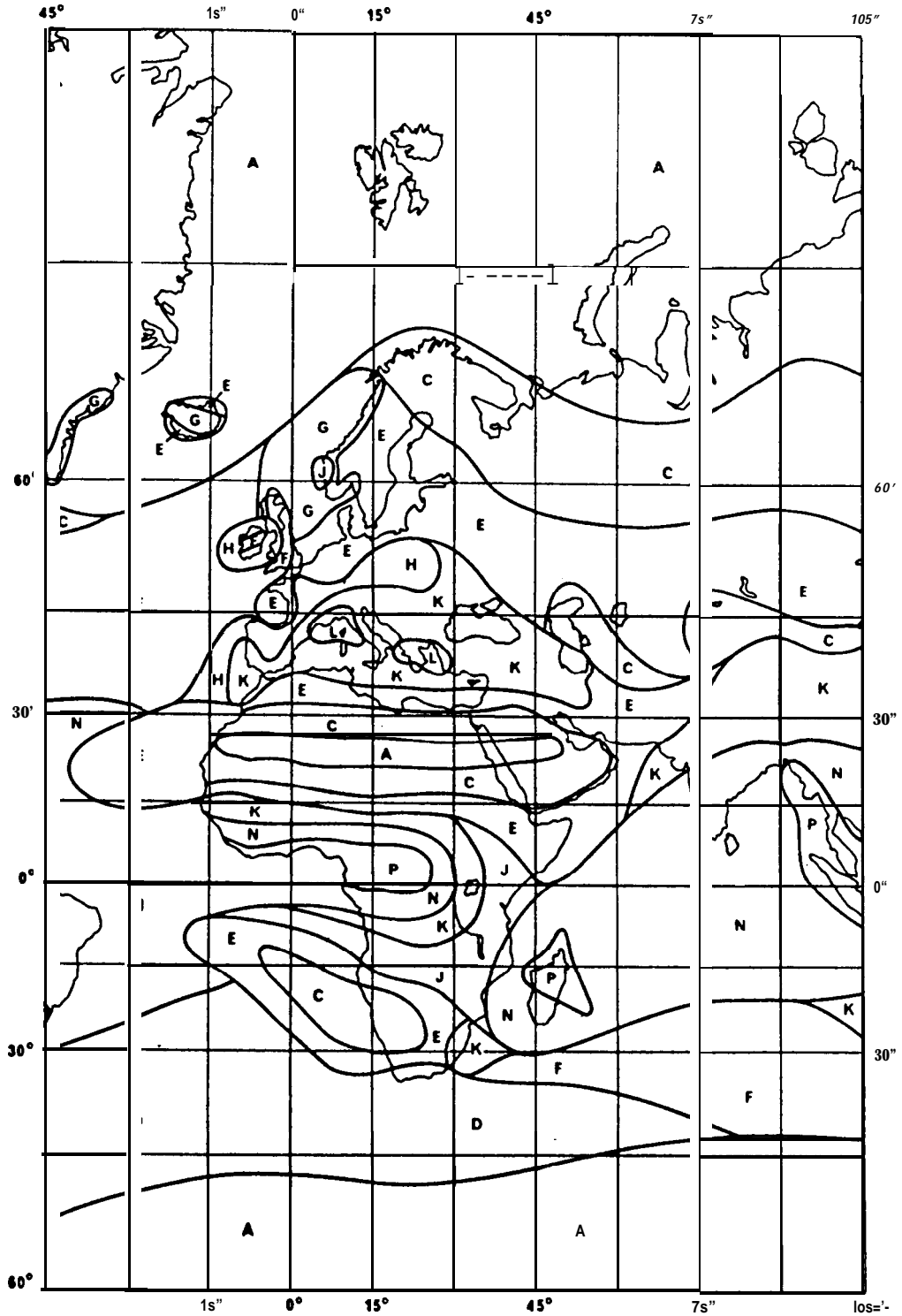


Figure 3.6-1. CCIR Rain Climate Zones (Sheet 2 of 3)

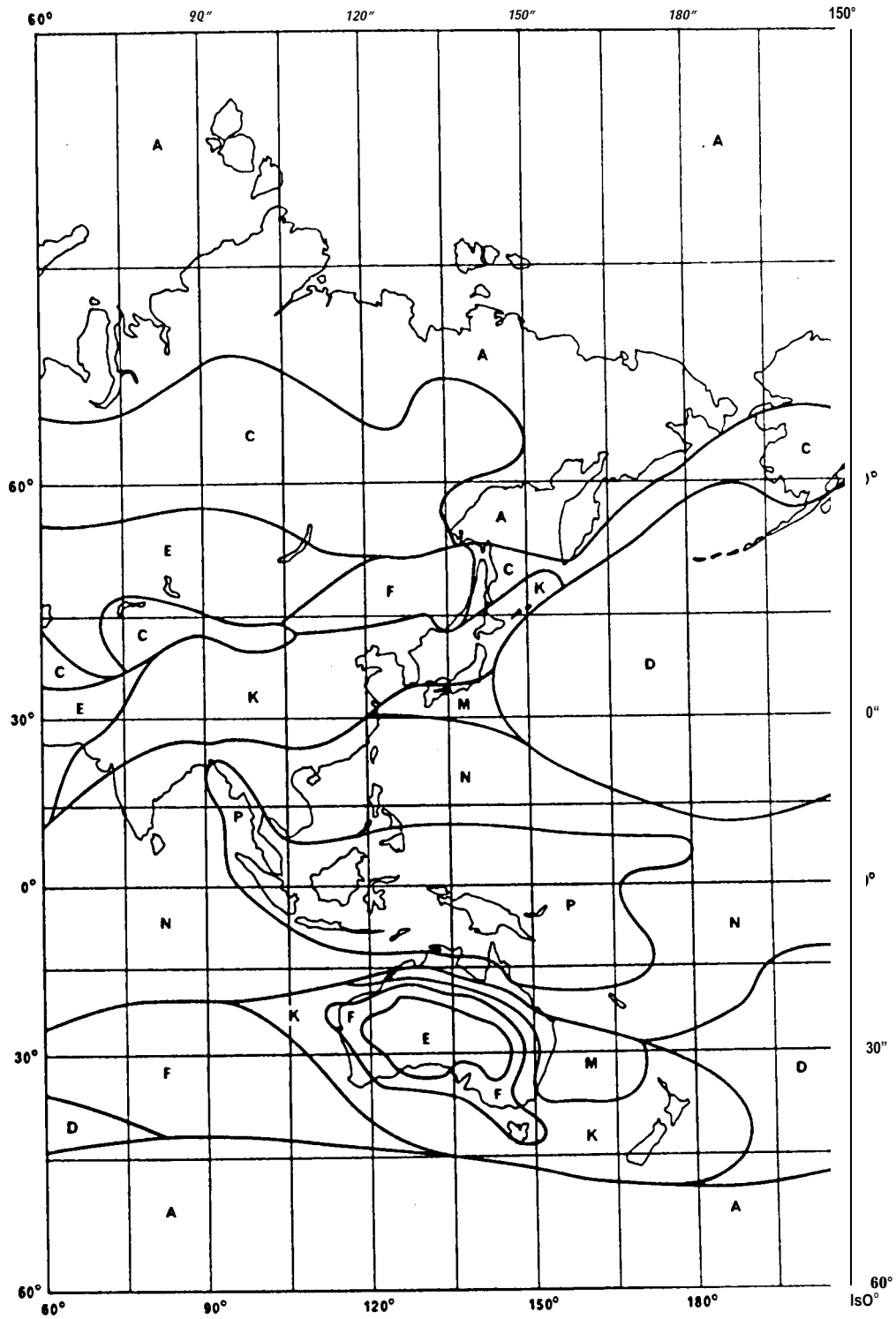


Figure 3.6-1. CCIR Rain Climate Zones (Sheet 3 of 3)

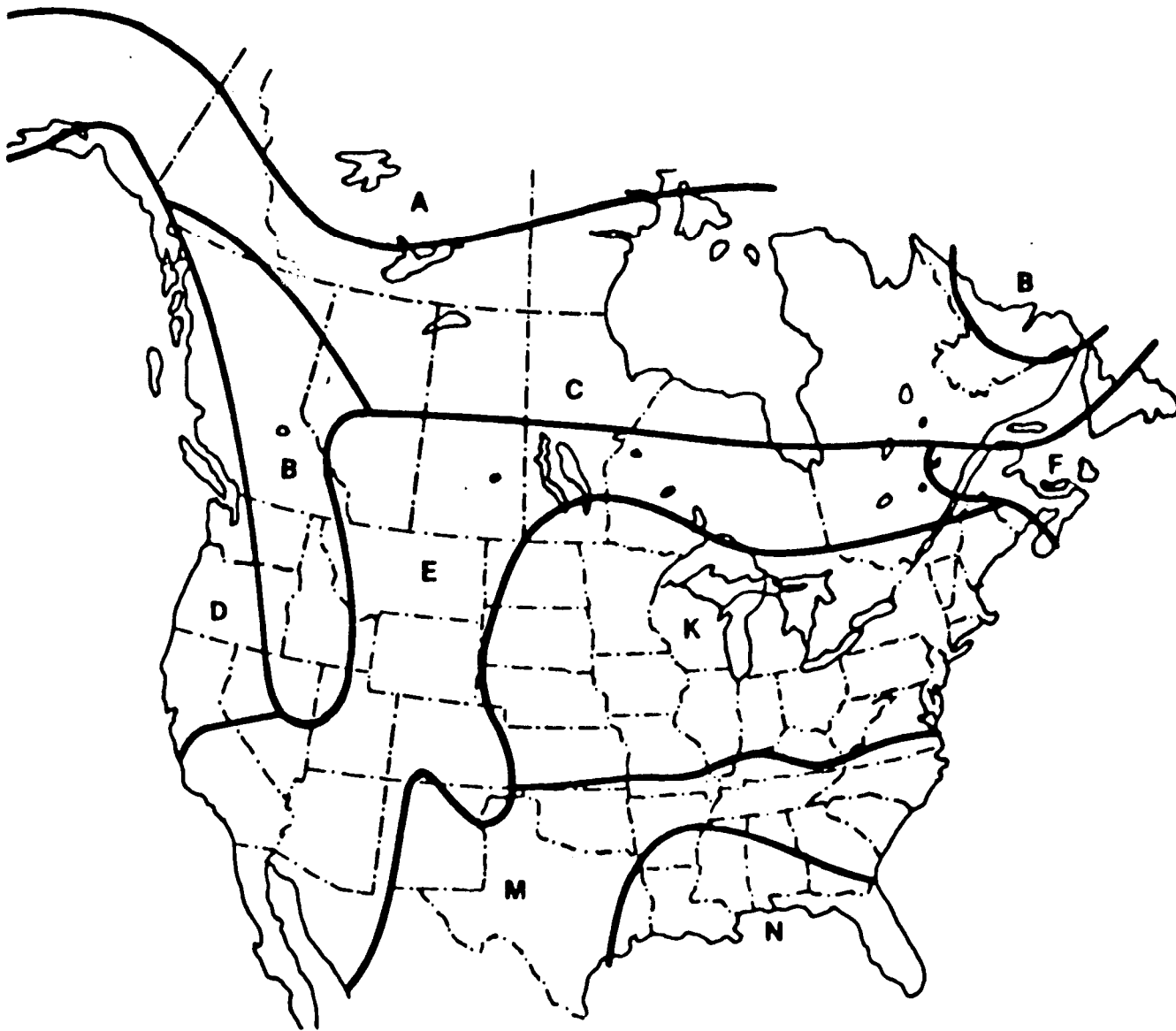


Figure 3.6-2. CCIR Rain Climatic Zones for the Continental United States and Canada

Table 3.6-1. Rainfall Intensity Exceeded (mm/h) for CCIR Rain Climatic Zones

% Time	A	B	C	D	E	F	G	H	J	K	L	M	N	P
1.0 -	<0.5	1	2	3	1	2	3	2	8	2	2	4	5	12
0.3	1	2	3	5	3	4	7	4	13	6	7	11	15	34
0*1	2	3	5	8	6	8	12	10	20	12	15	22	35	65
0*03	5	6	9	13	12	15	20	18	28	23	33	40	65	105
0.01	8	12	15	19	22	28	30	32	35	42	60	63	95	145
0.003	14	21	26	29	41	54	45	55	45	70	105	95	1409	200
0.001	22	32	42	42	70	78	65	83	55	100	150	120	180	250

The CCIR also provides maps showing isometric rain rate contours for the 0.01 percent exceedance value, which will be used in the attenuation model procedure. This isometric map is given as Figure 3.6-3.

The CCIR model assumes that the horizontal extent of the rain is coincident with the ambient 0°C isotherm height, which will vary with location, season of the year, time of day, etc. An average value of the 0°C isotherm weight is used in the CCIR model, obtained from,

$$\begin{aligned}
 h_r &= 4.0 && \text{for } 0 < \phi < 36^\circ \\
 &= 4.0 - 0.075 (\phi - 36) && \text{for } \phi \geq 36^\circ
 \end{aligned}
 \tag{3.6-1}$$

where ϕ is the latitude of the location of interest, in degrees N or S.

This estimate is recognized as having high variability, particularly at higher latitudes, and for locations where the significant rain accumulation occurs at other than the summer rainy season.

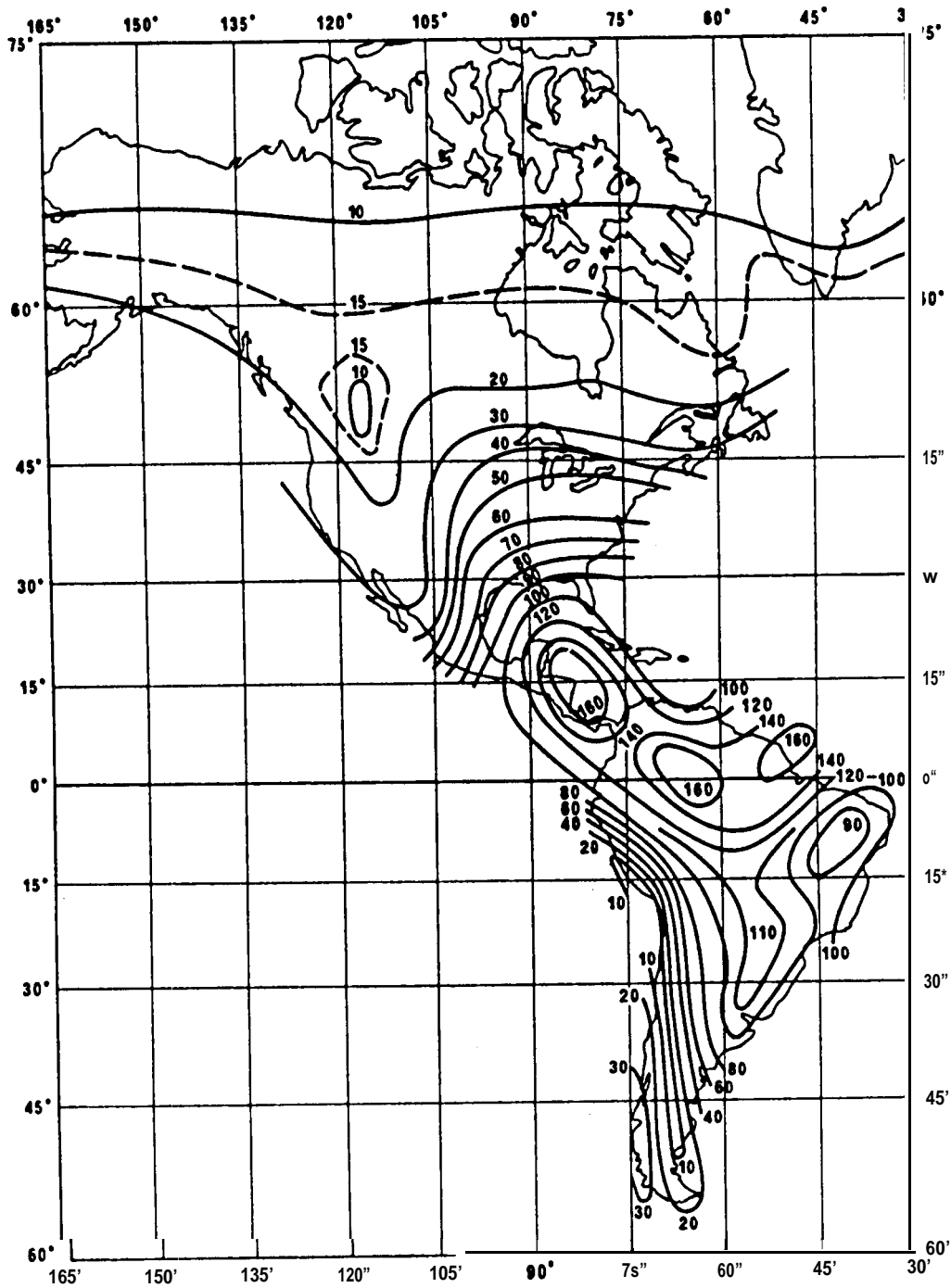


Figure 3.6-3. Contours of Rain Rate Exceeded for 0.01% of the Time (mm/hr) (Sheet 1 of 3)

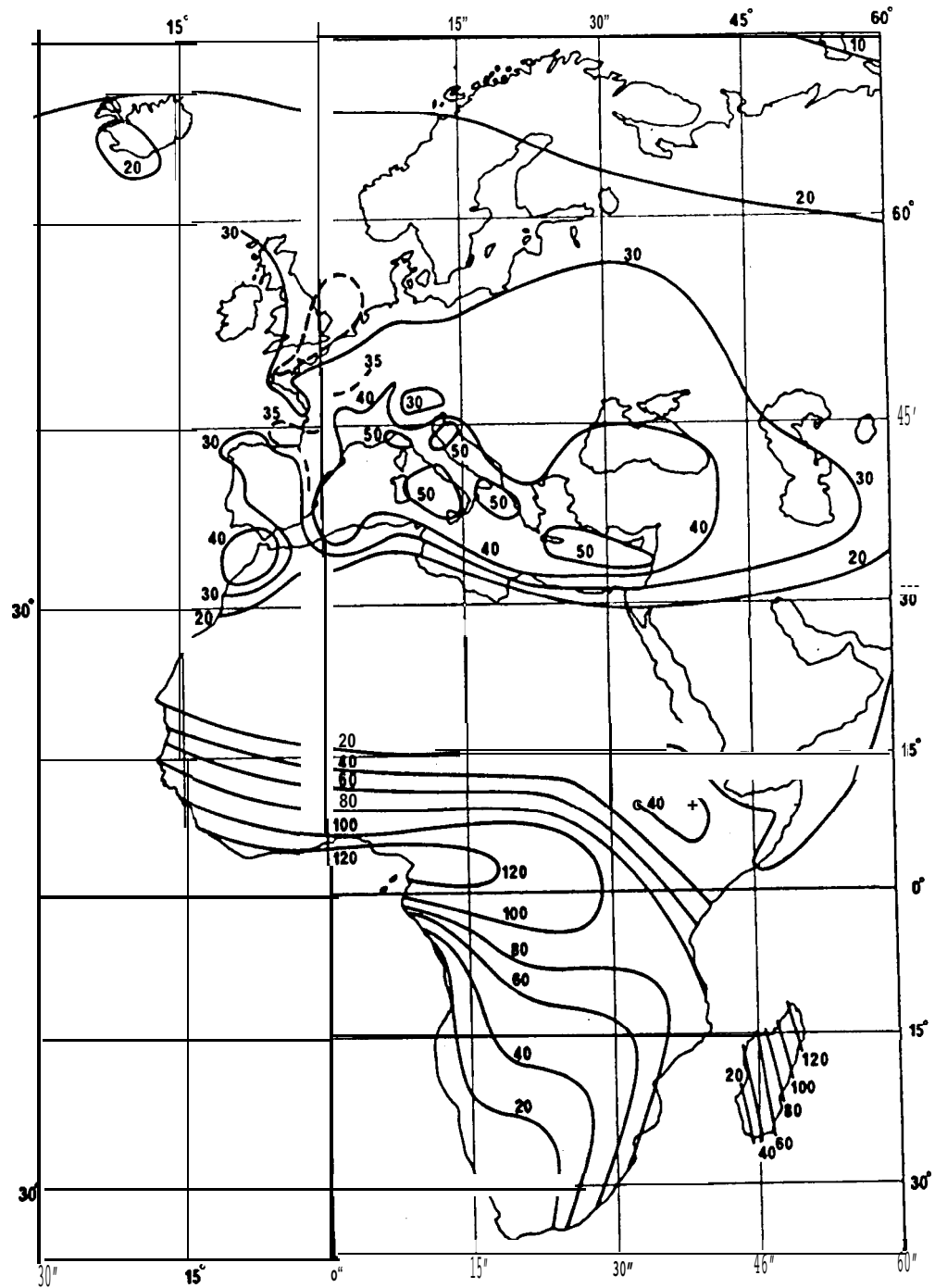


Figure 3.6-3. Contours of Rain Rate Exceeded for 0.01% of the Time (mm/hr) (Sheet 2 of 3)

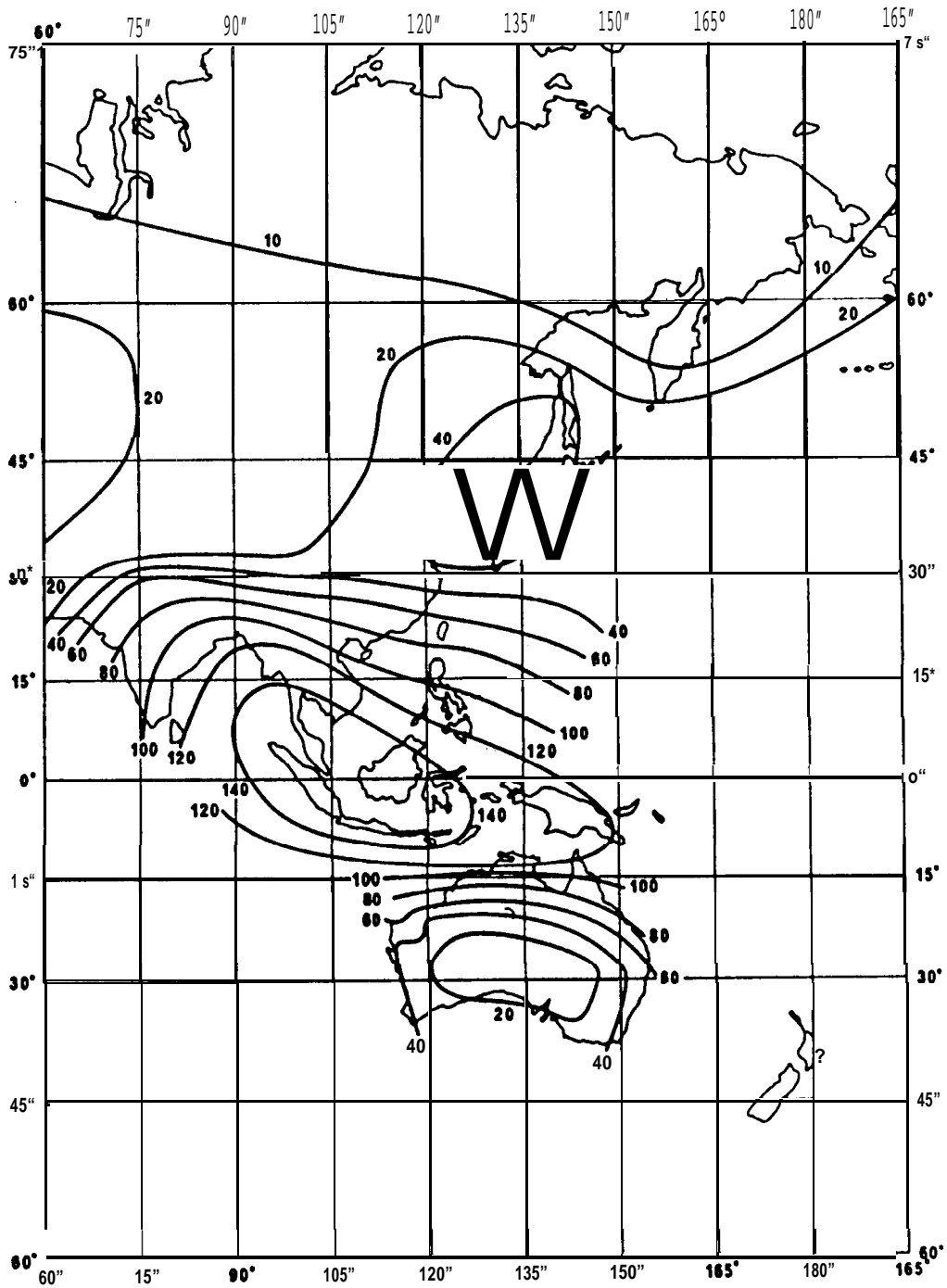


Figure 3.6-3. Contours of Rain Rate Exceeded for 0.01% of -
the Time (mm/hr) (Sheet 3 of 3)

3.6.2 CCIR Attenuation Model

The CCIR attenuation prediction requires the following input parameters:

- . frequency (**GHz**)
- latitude of earth station (degrees),
- height above mean sea level of earth station (km)
- elevation angle to the satellite (degrees), and
- . point rainfall rate for the location for 0.01% of an average year (mm/h).

The rain height, h_r , is determined from the latitude by equation (3.6-1) above. The projected path length on the earth's surface, L_g , and the slant path length through the rain, L_s , are geometrically determined from h_r , the elevation angle, and the height above sea level. A slant path length reduction factor is then applied to account for the horizontal non-uniformity of rain for the 0.01% of the time condition. The reduction factor, r_p , is given by:

$$r_p = \frac{1}{1 + 0.045 L_g} \quad (3.6-2)$$

The product of L_s and r_p is the effective path length through rain for 0.01% of the time.

The specific attenuation for 0.01% of an average year, $\alpha_{0.01}$, in dB/km, is determined from the power-law relationship with rain rate, [see equation (2.3-5)], utilizing the rain rate at 0.01% of the year from locally measured data (preferred)? or from Table 3.6-1. The power law coefficients at the frequency and polarization of interest can be obtained from Table 2.3-2, Table 2.3-3, or other

suitable sources. The specific attenuation in the CCIR model is assumed to be constant up to the rain height.

The attenuation exceeded for 0.01% of an average year is then obtained from,

$$A_{0.01} = a_{0.01} L_{srp} \text{ dB} \quad (3.6-3)$$

The attenuation exceeded for other percentages of an average year, p , in the range 0.001% to 1%, are then determined from $A_{0.01}$ by,

$$A_p = 0.012 A_{0.01} p^{-(0.546 + 0.043 \log p)} \text{ dB} \quad (3.6-4)$$

The **CCIR** reports that when the above prediction method was tested with measured data for latitudes above 30°, the prediction was found to be in agreement at the 0.01% point to within 10%, with a standard deviation of 30%, when used with simultaneous rain rate measurements. Between latitudes of 20° and 30° the prediction method consistently over-estimated the attenuation by a factor of about one-third. When local measured rain rate statistics are used instead of the average year values given in the **CCIR** climatic zone tables, the errors are found in general to be less, at all latitudes (**CCIR-1986a**).

The detailed step-by-step procedure for the **CCIR** attenuation prediction model, including an example application, is presented in Section 6.3 of the handbook.

3.7 THE LIN MODEL

3.7.1 Empirical Formulas

The set of empirical formulas presented here for earth-satellite path attenuation is an extension of those obtained previously for terrestrial microwave radio paths (**Lin-1978**). In the case of terrestrial paths, the calculation of the expected rain attenuation

distribution from a long term (20 years) distribution of 5-minute point rain rates has been accomplished using empirical formulas deduced from available rain rate and rain attenuation data measured on nine 11 GHz radio paths (5-43 km) at five different U.S. locations (Lin-1977).

These empirical formulas for terrestrial paths, are (Lin's notation (1978) reverses the role of a and β)

$$a(R) = a R^b \text{ dB/km} \quad (3.7-1)$$

$$\beta(R,L) = a(R) \left[1 + \frac{1}{\bar{L}(R)} \right]^{-1} L \quad (3.7-2)$$

where

$$\bar{L}(R) = \frac{2636}{R - 6.2} \text{ m} \quad (3.7-3)$$

R is the 5-minute point rain rate in mm/h, L is the radio path length in km, $\beta(R,L)$ is the path rain attenuation in dB at the same probability level as that of R , and the parameters a and b are functions (Setzer-1970, Chu-1974, Saleh-1978) of the radio frequency, as shown in Figure 3.71. (Strictly speaking, the parameters a and b are also functions of wave polarization.)

3.7.2 Rain Path Averaging

If the rain rates were uniform over a radio path of length L , the path rain attenuation $\beta(R,L)$ would be simply $a(R) \cdot L$, representing a linear relationship between β and L . However, actual rainfalls are not uniform over the entire radio path, and therefore the increase of $\beta(R,L)$ with L is nonlinear.

Two factors in the empirical method account for the radio path averaging effect. First, the method is based upon the long term distribution of 5-minute point rain rates in which the 5-minute time averaging partially accounts for the fact that the radio path performs a spatial averaging of non-uniform rain rates (Freeny and **Gabbe-1969**, **Drufuca** and **Zawadzki-1973**, **Bussey-1950**). A 5-minute average of the rain rate seen at a point corresponds to spatially averaging approximately 2.1 km of vertically variable rain **rates**, assuming 7 meters/second average descent velocity of rain drops.

Figure 3.7-2 shows how the point rain rate distribution, from two years of measurements at Palmetto, Georgia, depends on the average time intervals (range: 0.5-60 minutes). The probability of a 5-minute rain rate exceeding the 40 mm/h threshold is 1/2 that of a 0.5-minute rain rate exceeding the same threshold. From another viewpoint, increasing the averaging time interval from 0.5 to 5 minutes reduces the 0.01 percentile (i.e., 53 minutes/year) rain rate from 87 to 58 mm/h.

However, since most radio paths of interest are longer than 2.1 km, the fixed 5-minute average interval cannot adequately account for all the path length variations. This deficiency is compensated for by the factor

$$\left[1 + \frac{1}{L(R)} \right]^{-1} \quad (3.7-4)$$

In other words, the auxiliary nonlinear factor represents the empirical ratio between the 5-minute point rain rate R and the radio path average rain rate $R_{av}(L)$ at the same probability level. Since the significant difference between the 5-minute point rain rate and the 0.5-minute point rain rate in Figure 3.7-2 already accounts for the major portion of the difference between the radio path average rain rate $R_{av}(L)$ and the 0.5-minute point rain rate, the auxiliary factor is a weak nonlinear function of L . Obviously, many different analytic functions can be used to approximate this mildly nonlinear

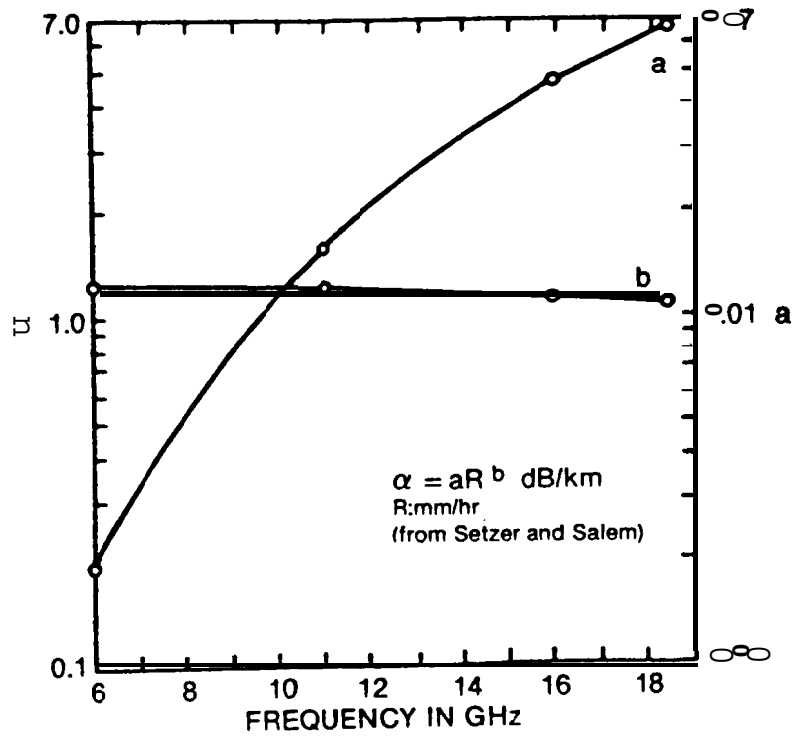


Figure 3.7-1. Dependence of Parameters a and b on the Radio Frequency

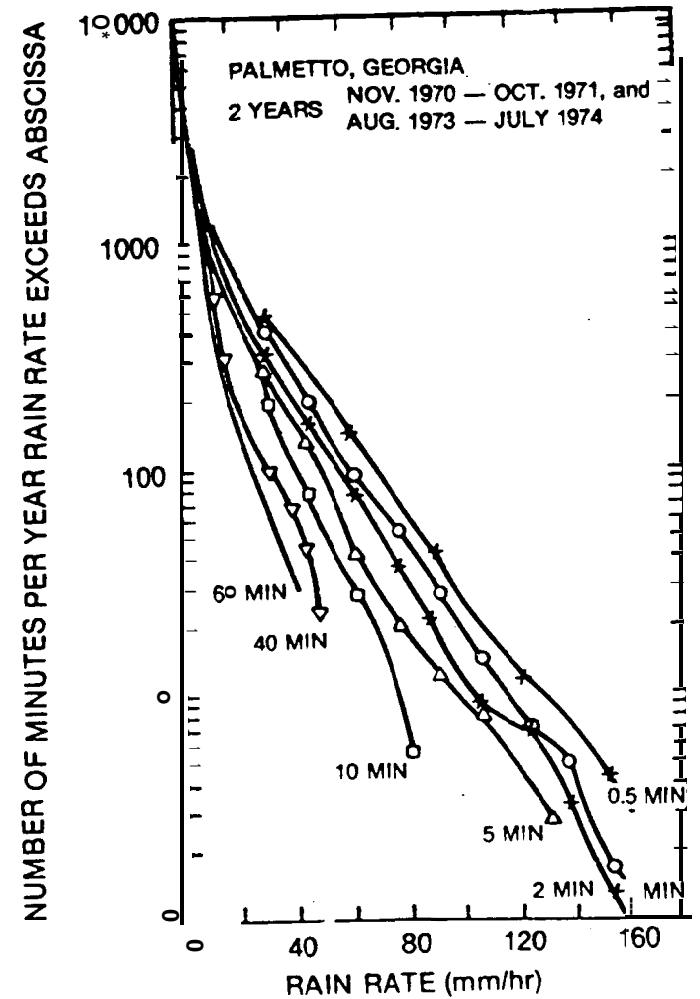


Figure 3.7-2. Dependence of Rain Rate Distribution on Tipping Bucket Rain Gauge Integration Time From Two Years of Measurement at Palmetto, Georgia

behavior. The single parameter function is selected for its simplicity. The adequacy of this simple approximation is supported by the rain rate and rain attenuation data measured on nine, 11-GHz, terrestrial radio paths at five U.S. locations (Lin-1977).

3.7.3 Earth-Satellite Path Legend

To extend the method to earth-satellite paths, let H be the long-term average height of the freezing level in the atmosphere, measured relative to sea level. The effective average length of the earth-satellite path affected by rain is then

$$L = (H - H_g) / \sin \theta \quad (3.7-5)$$

where θ is the satellite elevation angle as viewed from the earth station, and H_g is the ground elevation measured from the sea level. The radar measurements of rainfall reflectivity at Wallops Island, Virginia indicate that on the average rainy day (CCIR-1977)

$$H \approx 4 \text{ km} \quad (3.7-6)$$

Thus given the elevation angle θ , the ground elevation H_g and the distribution of 5-minute point rain rates, we can calculate the rain attenuation distribution on the earth-satellite path through the use of equations 3.7-1, 2 and 5.

Notice that equation 3.7-5 implies that the path rain attenuation (R, L) varies exactly as the cosecant of the elevation angle θ with this simple extension of the terrestrial model. Also note that these simple formulas are valid only on the long term average. The short term relationships between the surface point rain rate and the earth-satellite path rain **attenuation**, on a **storm-by-storm** basis, have been observed to be erratic and difficult to predict.

3.8 THE SIMPLE ATTENUATION MODEL (SAM)

The Virginia Polytechnic Institute and State University (VPI&SU), Blacksburg, VA, has been engaged for several years in the

development of rain attenuation models and related measurement programs. Several iterations of a quasi-physical **model** of rain attenuation on a slant path have been provided. One of the earliest versions of a comprehensive rain attenuation prediction model was the **Piecewise** Uniform Rain Rate Model, (Persinger, et al-1980) [described in detail in the previous (3rd) edition of this handbook]. The Piecewise Uniform Model accounted for the nonuniform spatial characteristics of rain with two simplifying assumptions: a) the spatial rain rate distribution is uniform for low rain rates, and b) as peak rain rate increases, the rain rate distribution becomes increasingly nonuniform.

The Piecewise Uniform Model was later extended with an expanded global data base to an exponential shaped rain rake profile (**Stutzman** and Dishman - 1982, 1984), and was called the Simple Attenuation Model (SAM). The model was further modified to include the effects of rain depolarization and an even larger data base (**Stutzman** and Yen, 1986). This latest version of the SAM will be described here.

The SAM is a **semiempirical** model that describes the spatial rainfall along a slant path ℓ by:

$$\begin{aligned}
 R(\ell) &= R_0 && R_0 \leq 10 \text{ mm/h} \\
 &= R_0 \exp[-\lambda \ln(R_0/10) \ell \cos \beta] && R_0 > 10 \text{ mm/h}
 \end{aligned}
 \tag{3.8-1}$$

where

$$\ell \leq L, \quad L = (H_e - H_0)/\sin \beta \tag{3.8-2}$$

and

R_0 is the point rainfall rate in mm/h,
 H_0 is the earth station altitude in km,
 H_e is the effective rain height in km,
 β is the slant path elevation angle, and
 λ is an empirical developed parameter
controlling the rate of decay of the horizontal profile.

The effective rain height is approximated by

$$\begin{aligned}
 H_e &= H_i & R_o &\leq 10 \text{ mm/h} & (3.8-3) \\
 &= H_i + \log(R_o/10) & R_o &> 10 \text{ mm/h}
 \end{aligned}$$

where H_i is the 0°C isotherm height in km. The seasonal average is obtained from (Crane-1978),

$$\begin{aligned}
 H_i &= 4.8 & \& \leq 30^\circ \\
 &= 7.8 - 0.1\epsilon & \& > 30^\circ & (3.8-4)
 \end{aligned}$$

here ϵ is the station latitude, in degrees N or S.

The total attenuation due to a point rainfall rate R_o is found by integrating Eq (3.8-1) over the path L:

$$A(R_o) = aR_o^b L \quad R_o \leq 10 \text{ mm/h} \quad (3.8-5)$$

$$A(R_o) = aR_o^b \frac{1 - \exp[-b\lambda \ln(R_o/10) L \cos \beta]}{b\lambda \ln(R_o/10) \cos \beta}$$

$$R_o > 10 \text{ mm/h}$$

An evaluation of 36 data sets in the expanded VPI&SU data base for which both attenuation and rain rate data were available found that a value of

$$A = 1/14 \quad (3.8-6)$$

gave the best fit to the data. The functional dependence of A is such that large changes do not produce changes in attenuation.

The revised SAM model was found by its authors to give equal to or slightly better predictions than the CCIR or the Global prediction models, for the available data base (Stutzman and Yon - 1986). Figure 3.8-1 shows a comparison of the models for 64 global data sets. Predictions are based on rain rates calculated from the CCIR rain rate model except for the Global Model which uses the Global rain rate model. Mean deviation and standard deviation of predicted attenuation as a percent based : . measured attenuation are shown. Figure 3.8-2 shows a similar comparison for 31 long term

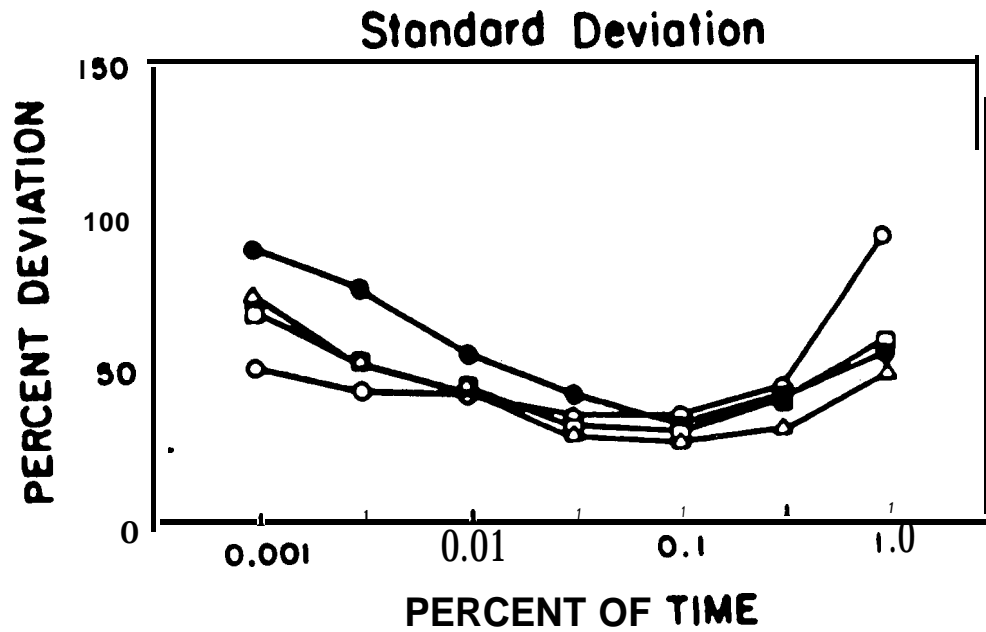
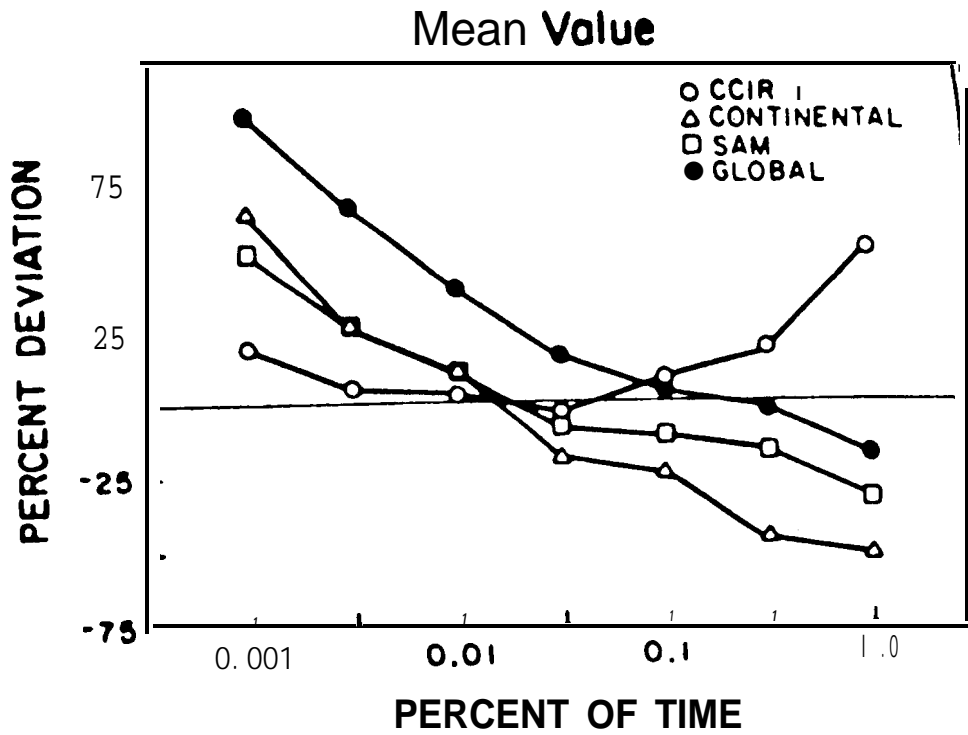


Figure 3.8-1. Comparison of the SAM model with the CCIR and Global models, for 62 measured data sets

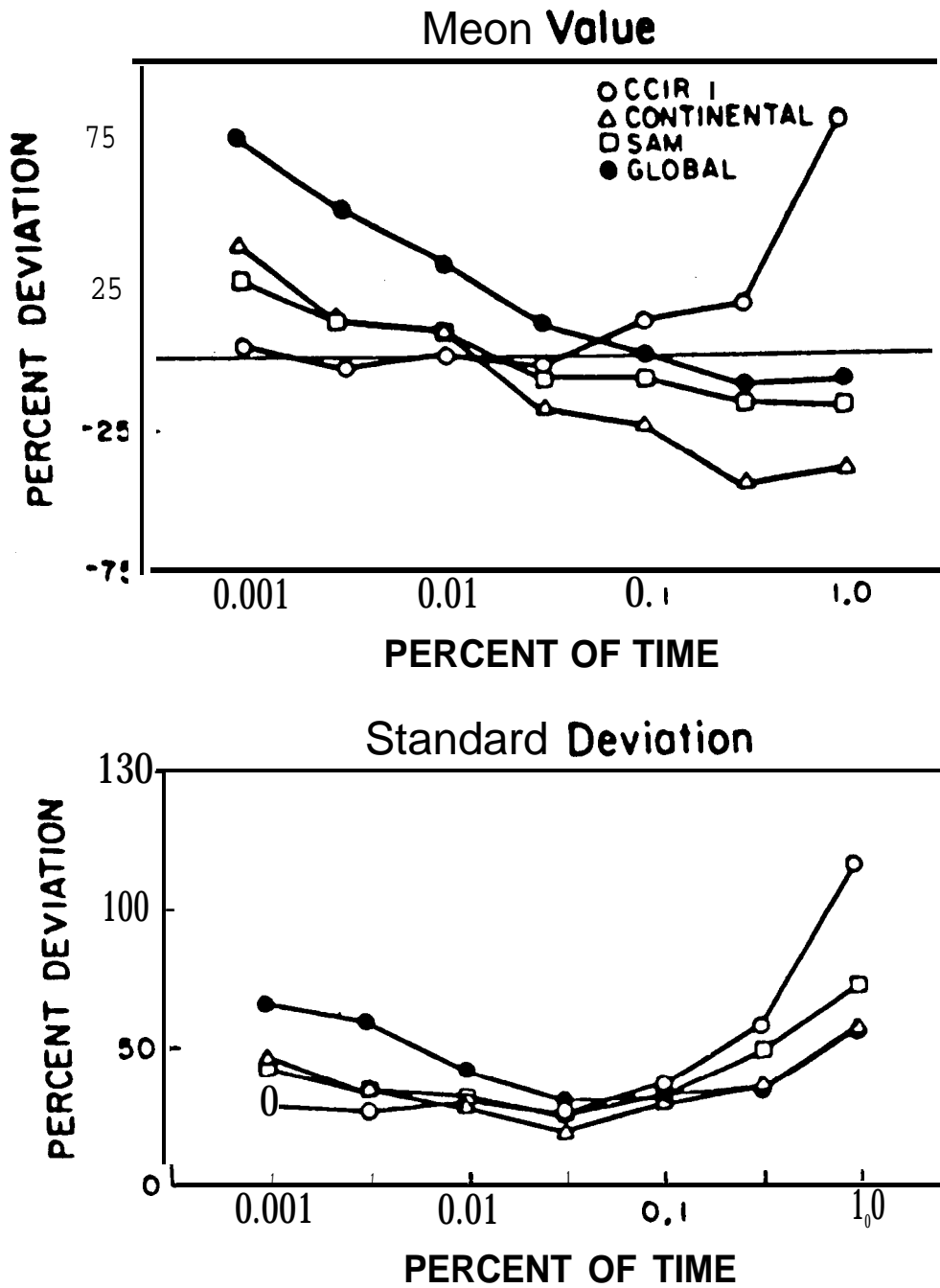


Figure 3.8-2. Comparison of the SAM model with the **CCIR** and **Global** models, for 32 long term (two years or more) measured data sets

(two years or more) data sets from the data base. All four models give better predictions for **long** term data sets, as expected, since" they are more representative of average rain **behavior**, for which the models are based.

3.9 THE EFFECTIVE PATH LENGTH CONCEPT

3.9.1 Definition of Effective Path Length

The effective path length L_e is usually defined as that parameter which relates the specific attenuation to the total attenuation along the earth-space path. Mathematically it is written

$$A = \alpha R^b L_e \quad (3.9-1)$$

Alternatively, L_e is the hypothetical path length of uniform rain rate R which will produce the same total path attenuation as the real varying rain rate does along the path. The form of L_e and the technique employed for its derivation has been quite variable. For example, in some cases it is termed effective path length and in others the path averaging factor.

Since rains are not usually uniform over the extent of the storm (**rain cells** of higher rain rates are small compared to the extent of the storm), the total attenuation is

$$A = \int_0^L \alpha_l dl \quad (3.9-2)$$

where A is the total attenuation at a given frequency and time through the **storm** of extent L along the path l . The factor α_l is a "high resolution" specific attenuation depending on the rain rate at each point along the path. The effective path length in kilometers

$$L_e = \frac{A}{a_{avg}} \quad (3.9-3)$$

is where a_{avg} is an analytically determined attenuation per kilometer assuming a uniform average rain rate. The average rain rate is based on rain rate measurements taken over a long period of time. The measured attenuation is also indirectly a function of average rain rate. Measured attenuation and measured rain rate data are compared on an equal probability of occurrence basis over a long time base. This removes the instantaneous time dependence of the measurements. Note that if rain rate is not a function of length l , then $A = a_{avg}L$ and the effective path length would equal the physical rain extent L . This is one limit which occurs for low rain rates. For example, for stratiform rains the rain rate is nearly spatially uniform.

3.9.2 Frequency Dependence of Effective Path Length

Some frequency dependence to the effective path length has been observed at higher rain rates. To investigate the frequency dependence of L_e consider the ratio of two L_e 's for two frequencies f_1 and f_2 . Namely,

$$\frac{L_e(f_1)}{L_e(f_2)} = \frac{\int_0^L a_1(f_2) dl}{\int_0^L a_1(f_1) dl} = r_p r_m^{-1} \quad (3.9-4)$$

where r_m is the ratio of the measured attenuations, and r_p is the ratio of the predicted attenuations assuming uniform rain conditions, which is also the ratio of predicted specific attenuations. For the effective path length to be independent of frequency r_m must equal r_p and the effective path length versus-rain rate must be identical for the two frequencies. Experimental results shown in Figure 3.9-1 demonstrate that for two frequencies

(19 and 28 GHz) and rain rates exceeding one inch per hour the effective path length of the higher frequency is as much as 20% longer than the lower frequency. This is an effect which must be considered when frequency scaling attenuation measurements over a wide- frequency range.

The frequency dependence of effective path length shown in Figure 3.9-1 arises from the nonuniformity of rain along the propagation path in combination with the nonlinear dependence of the specific attenuation on rain rate. Using the definition in equation 3.9-1, the relation (**Kheirallah, et al-1980**)

$$L_e(f_2) = L_e(f_1)^{b(f_2)/b(f_1)} \quad (3.9-5)$$

has been derived. This relation has been compared with some experimental data and appears to apply best to the low frequency (4 to 10 GHz) data for high rain rates (exceeding 25 mm/h).

Kheirallah, et al (1980) attributes this to the relatively significant effects of cloud attenuation at higher frequencies and low rain rates.

Rewriting equation 3.9-5 one has

$$[L_e(f_1)]^{1/b(f_1)} = [L_e(f_2)]^{1/b(f_2)} = L_e' \quad (3.9-6)$$

L_e' is defined as the normalized effective path length and is much less dependent on frequency than L_e . **Kheirallah, et al (1980)** suggests that for small percentages of time for which rain attenuation dominates, data sets should be expressed in terms of L_e' before data at various frequencies and elevation angles are combined.

3.9.3 Effective Path Length Versus Measurement Period

Experimentally determined effective path lengths for varying measurement periods (such as annual and worst month) show a high variability. For **example**, in Figure 3.9-2 each curve was developed from equal probability attenuation - rain rate measurements for the

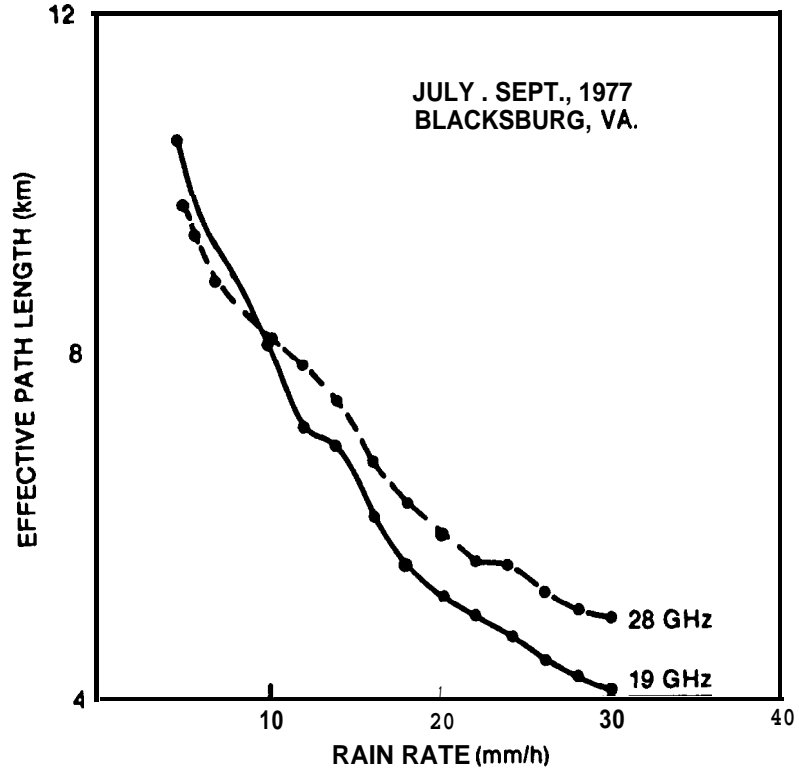


Figure 3.9-1. Effective Path Lengths for the VPI & SU COMSTAR 19 and 28 GHz Systems

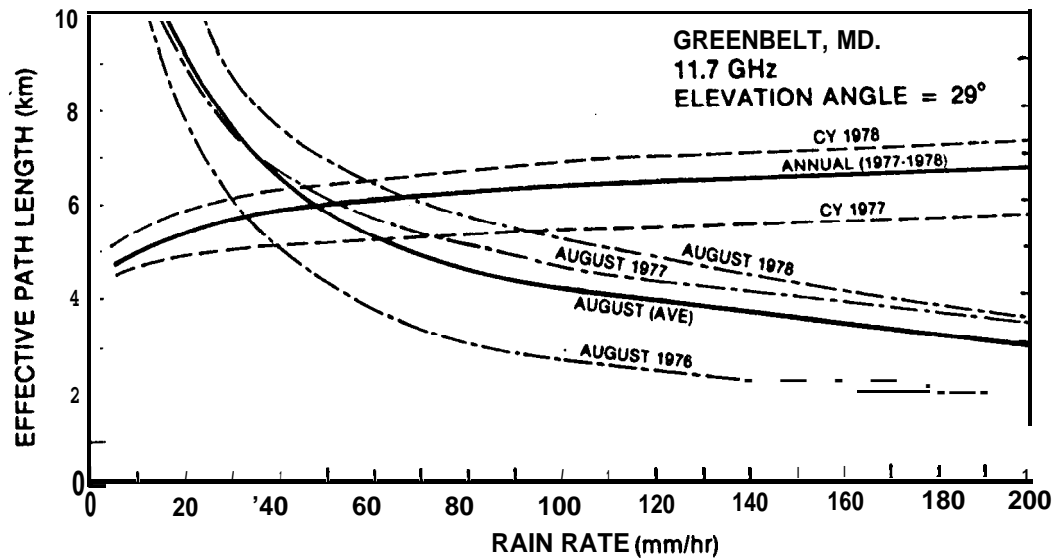


Figure 3.9-2. Effective Path Length for Annual & Worst Month Periods

period indicated. Two trends are apparent, First, the monthly curves show a decreasing path length with increasing rain rate, and second, the annual curves show a path length which increases slightly with rain rate. The first effect arises because the high rain rate events in August are primarily convective storms with intense localized rain rates. The second effect is probably accounted for because the winter rains in Maryland are more uniform in nature and the zero degree isotherm is significantly lower in winter. For this case L_e approaches L for cold weather low rain rate events. However, this effect has not always been observed (see below) and probably indicates that regions with low rainfall during the cold weather months will show a rain rate dependence to L_e similar to that for the worst month.

3.9.4 Comparison of Effective Length Factors

Several of the attenuation models utilize a factor easily related to L_e . It is of interest to compare these factors and determine their relative differences based on a similar set of assumptions. First consider the L_e factor in each model separately.

3.9.4.1 Dutton-Dougherty Model. This model does not explicitly employ an effective path length. An effective path length may be evaluated, however, and it has been by Dutton, et al (1982) for the purpose of comparison with the Global model. The relation between the effective path length given by the DD Model and the rain rate is a complex one, being determined by the liquid water content versus height function, $L(h)$, and the probability modification factor, F . There are two choices for $L(h)$, corresponding to stratiform and convective rain, and the model combines these for some time percentage values. Because a simple expression for L_e is not possible, no attempt is made here to define an effective path length for this model.

3.9.4.2 Global Model. Both forms of the Global model employ a term which can be related to the effective path length. For the path averaging technique (Global Prediction Model)

$$L_e = \frac{H}{\sin \theta} \gamma(D) R_p^{-d(D)} \quad (3.9-7)$$

where R_p is the point rain rate, H is the height of the 0°C isotherm, D is the basal distance and γ and δ are the path averaging factors defined in Section 3.4. For a 45° elevation angle at a sea-level ground station near 40°N latitude

$$L_e = 9.14 R_p^{-0.14} \text{km} \quad (3.9-8)$$

For the variable isotherm height form of the Global model,

$$L_e = \frac{1}{\cos \theta} \left[\frac{e^{UZb-1}}{Ub} - \frac{X^{be}YZb}{Yb} + \frac{X^{be}YDb}{Yb} \right] \quad (3.9-9)$$

where the terms are defined in Section 3.4.3.2. The value of L_e is a complex function of R_p since U , X , Y and Z (implicitly) are functions of R_p .

3.9.4.3 Two-Component Model. Two effective path lengths could be identified in the T-C Model: one for convective cellular rain and one for debris. Differing 0°C isotherm heights are computed for the two types of rain which form a basis for the differing effective path lengths. The lateral modeling of rain also differs for the two rain modes: cellular rain effective path length must be modified to include nearby debris contributions, whereas debris rain is assumed to be uniform. Thus, no attempt is made to identify a single parameter L_e in the T-C Model.

3.9.4.4 CCIR Model. The CCIR Model directly employs the concept of effective path length. The (corrected) 0°C isotherm height is used to define the vertical extent of rain. A slant path length reduction factor is used to adjust the physical path length through rain to **account** for the horizontal **non-uniformity** of rain. The resulting effective path length applies only for 0.01% of the time. The attenuation predictions for other time percentages are determined directly from the 0.01% value, without reverting to the path length. For this reason, the dependence of effective path length on rain rate is obscure.

3.9.4.5 Lin Model. The Lin model utilizes two techniques for obtaining the average path length. The first is to temporally average the instantaneous rain rate to five minute intervals. The effect of this averaging process in terms of the effective path length comparison is unclear. However, as will be shown, the other parameter agrees well with the results of other models. Specifically Lin (1978) finds that

$$L_e = \frac{4}{\sin \theta} \left[1 + \frac{4(R_p - 6.2)}{2636 \sin \theta} \right]^{-1}$$

(3.9-10)

$$= \frac{2636}{659 \sin \theta + R_p - 6.2}$$

At $\theta = 45$ degrees the result is

$$L_e = 2636(460 + R_p)^{-1}$$

(3.9-11)

3.9.4.6 Simple Attenuation Model (SAM). The simple attenuation model does not readily allow definition of a single L_e parameter. Therefore this parameter is not derived.

3.9.4.7 Experimental Measurements. **Ippolito** (1978) has employed over sixty months of long term attenuation and rain rate statistics at 11.7, 15, 20 and 30 GHz to derive an effective path length based on experimental measures. The result is

$$L_e = \frac{9.065}{\sin \theta} R_p^{-0.296} \text{ km} \quad (3.9-12)$$

for elevation angles from 20 to 90 degrees. At 45 degrees elevation angle

$$L_e = 12.82 R_p^{-0.296} \quad (3.9-13)$$

3.9.4.8 Comparison of Effective Path Lengths. Assuming a ground station at sea level, 40 degrees North latitude and observing at 45 degrees elevation angle, the L_e factors are plotted in Figure 3.9-3 for the two forms of the Global model, the Lin model and the experimental results of **Ippolito** (1978) and **CTS** results (Ippolito-1979). The latter experimental results (labeled $L_e, \text{exp}(11.7\text{GHz})$ in Figure 3.9-3) were scaled from the 29 degree elevation angle measurements made at **Greenbelt**, MD to CTS, to 45 degrees using the ratio of the **cosecants** of the two angles. The original data is the annual curve for 1977 and 1978 shown in Figure 3.9-2. This data is the longest set of continuous, single-site effective path length data published to date for **CTS** and therefore more weight should be given this curve.

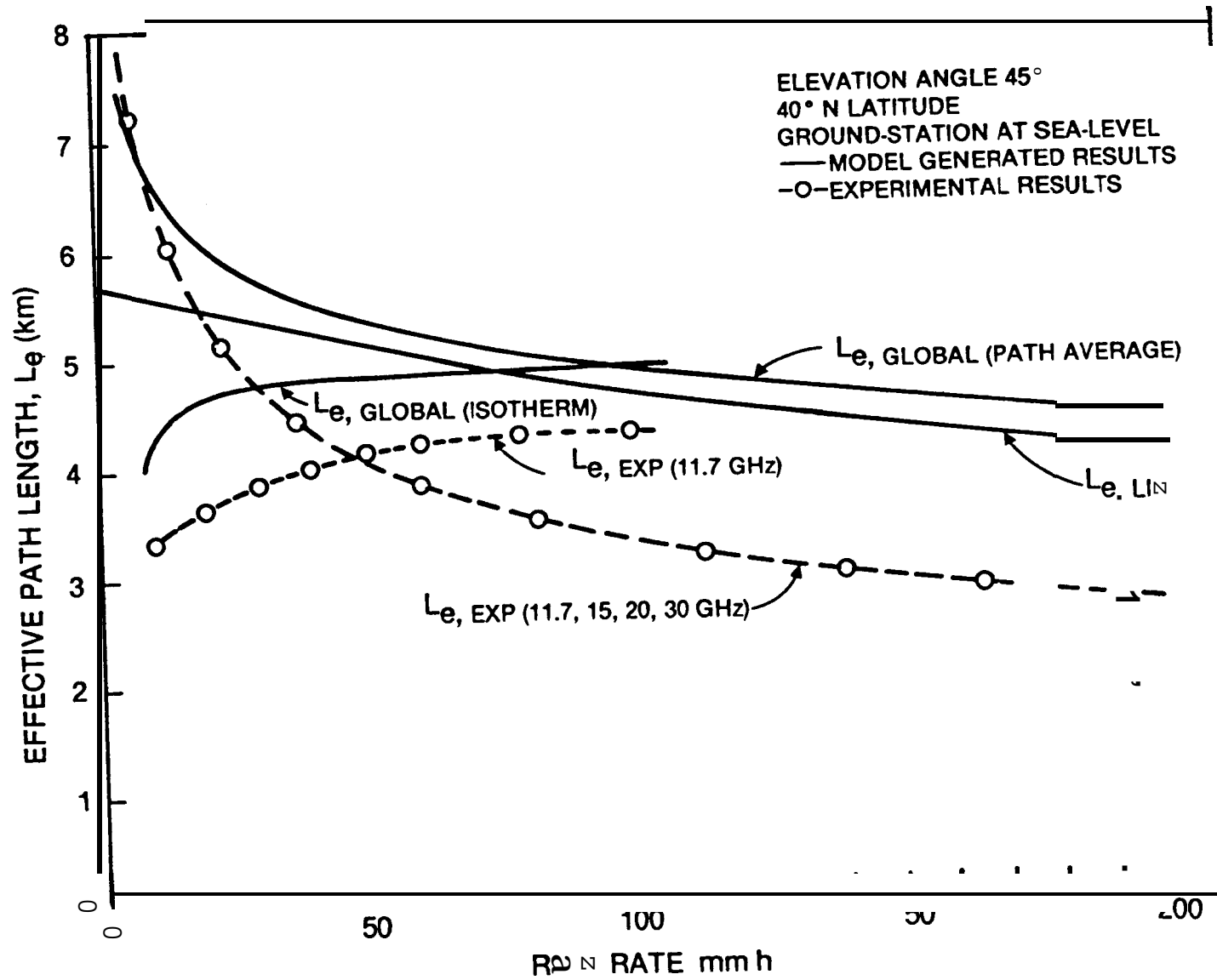


Figure 3.9-3. A Comparison of Effective Path Lengths

The most important result in Figure 3.9-3 is that the use of an effective path length between 4 and 5 kilometers is reasonable. A significant variation occurs below 30 mm/h which may arise due to the presence of winter rains, but this remains unproven. Fortunately for most design problems the most accurate estimates of effective path length are required for annual percentages in the range from 0.01 and 0.001 percent of a year, and in this range both the experimental and model-generated effective path lengths are approximately 4 to 5 km. However, assuming a ± 1 km error bound on L_e the error in estimating L_e is about ± 1 dB. If L_e is directly related to the total attenuation, at least a ± 1 dB error bound must be placed on the estimate of the path attenuation. This error bound will increase as the elevation angle decreases.

3.10 REFERENCES

- Barry, **R.C.** and **R.J. Chorley** (1970), Atmosphere, Weather and Climate, **Holt, Reinhart and Winston, Inc.**, New York, p. 205.
- Bussey, **H.E.** (1950), "Microwave Attenuation Statistics Estimated from Rainfall and Water Vapor Statistics," Proc. IRE, Vol. 38, pp. 781-785.
- CCIR** (1977), "Influence of the Non-Ionized Atmosphere on Wave Propagation," **CCIR Study Groups Period 1974-1978**, DOC. 5/169-E, May 10 United States of America, Modification to Report 233-3 (REV. 76).
- CCIR** (1978), "Propagation in Non-Ionized Media", **Volume V, XIV Plenary Session, Kyoto, Japan.**
- CCIR** (1978a), Special Preparatory Meeting (**WARC-79**) Documents.
- CCIR** (1982a), "Propagation Data Required for Space Telecommunications Systems," Report 564-2, in Volume V, Recommendations and Reports of the CCIR - 1982, International Telecommunications Union, Geneva.
- CCIR (1982b)**, "Prediction of Attenuation Due to Rain on an Earth-Space Path," **CCIR Interim Working Party (IWP) 5/2 Meeting**, June 1982, Geneva.
- CCIR (1982c)**, "Technical Bases for the Regional Administrative Radio Conference - 1983 for the Planning of the Broadcasting **Satellite** Service in Region 2," Report of the CCIR Conference Preparatory Meeting, **Geneva, 28 June - 9 July . 1982.**

- CCIR (1985a), "Radiometeorological Data," Report 5.63-2 (MOD F), Study Group 5 Inputs to XVth Plenary Assembly, Document 5/1017, 6 Nov. 1985.
- CCIR (1985b), "Propagation Data and Prediction Methods Required for Earth-Space Telecommunication Systems," Report 564-2 (Mod-F), Study Group 5 Inputs to XVth Plenary Assembly, Document 5/1040, 28 Nov. 1985.
- CCIR (1986a), "Radiometeorological Data," Report 563-3, in Volume v, Recommendations and Reports of the CCIR - 1986, International Telecommunications Union, Geneva.
- CCIR (1986b), "Propagation Data and Prediction Methods Required for Earth-Space Telecommunication Systems," Report 564-3, in Volume V, Recommendations and Reports of the CCIR - 1986, International Telecommunications Union, Geneva.
- Chu, T.S. (1974), "Rain Induced Cross-Polarization at Centimeter and Millimeter Wavelengths," B.S.T.J., Vol. 53, pp. 1559-1579.
- Crane, R.K. (1966), "Microwave Scattering Parameters for New England Rain," MIT Lincoln Laboratory Report 426, ASTIA Dec. AD-647798.
- Crane, R.K. and D.W. Blood (1979), "Handbook for the Estimation of Microwave Propagation Effects - Link Calculations for Earth-Space Paths," Environmental Research and Technology Rpt. No. 1, DoC. No. P-7376-TRL.
- Crane, R.K. (1978), "A Global Model for Rain Attenuation Prediction," Eascon Record, pp. 391-395.
- Crane, R.K. (1980a), "Prediction of Attenuation by Rain," IEEE Trans. Comm., Vol. COM-28, No. 9, pp. 1717-1733.
- Crane, R.K. (1980b), "Earth-Space and Terrestrial Microwave Propagation - Estimation of Rain Attenuation with the Global Model," ERT Technical Report P-A414-TR, prepared for NASA Headquarters under Contract NASW-3337 (October 1980).
- Crane, R.K. (1982), "A Two-Component Rain Model for the Prediction of Attenuation Statistics," Radio Science, Vol. 17, No. 6, pp. 1371-1387
- Dougherty, H.T. and E.J. Dutton (1978), "Estimating Year-to-Year Variability of Rainfall for Microwave Applications," IEEE Trans. Comm., Vol. COM-26, No. 8, PPO 1321-1324.

- Drufuca, G.** and **1.1. Zawadzki** (1973), "Statistics of Rain Gauge Records," Inter-Union Commission on Radio Meteorology (IUCRM) Colloquium on "The Fine Scale Structure of Precipitation and Electromagnetic Propagation" Nice, France, Conference Record, Vol. 2.
- Dutton, **E.J.** (1971), "A Meteorological Model for Use in the Study of Rainfall Effects on Atmospheric Radio Telecommunications " Off. **Telecomm.** Rpt. **OT/TRER-24**, NTIS No. **COM-75-10826/AS**, Springfield, Va.
- Dutton, **E.J.** (1977), "Earth-Space Attenuation Prediction Procedures at 4 to 16 **GHz**," Off. **Telcom.** Rpt. 77-123.
- Dutton, **E.J.** and **H.T. Dougherty** (1973), "Modeling the Effects of Clouds and Rain Upon Satellite-to-Ground System Performance," Off. **Telecom.** Report 73-5, NTIS No. COM-75-10950, Springfield, Va.
- Dutton, **E.J.** and **H.T. Dougherty** (1979), "Year-to-Year Variability of Rainfall for Microwave Applications in the U.S.A. ," IEEE Trans. Comm., Vol. **COM-27**, pp. 829-832.
- Dutton, **E.J.** and **H.T. Dougherty** (1984), "A Second Modeling Approach to Year-to-Year Rainfall Variability in the U.S.A. for Microwave/Millimeter Wave Applications," IEEE Trans. Comm., Vol. **COM-32**, No. 10, pp. 1145-1148.
- Dutton, E.J., H.T. Dougherty and R.F. Martin, Jr.** (1974), "Prediction of European Rainfall and Link Performance Coefficients at 8 to 30 **GHz**," Off. Telecom. , Dept. of Commerce, NTIS No. AD/A-000804, Springfield, Va.
- Dutton, **E.J., H.K. Kobayashi, and H.T. Dougherty** (1982), "An Improved Model for Earth-Space Microwave Attenuation Distribution Prediction," Radio Science, Vol. 17, No. 6, pp. 1360-1370.
- Freeny, **A.E.** and **J.D. Gable** (1969), "A Statistical Description of Intense Rainfall," B.S.T.J. , Vol. 48, No. 6, pp. 1789-1851.
- Goldhirsh, J.** and **I. Katz** (1979), "Useful Experimental Results for Earth-Satellite Rain Attenuation Modeling," IEEE Trans. Ant. Prop., Vol. **AP-27**, No. 3, pp. 413-415.
- Gray, **L.F.** and **M.P. Brown, Jr.** (1979), "Transmission Planning for the First U.S. Standard C (14/11-GHz) INTELSAT Earth Station," Comsat Tech. Rev., Vol. **9**, No. 1, pp. 61-89.

- Hyde, G. (1979), private communication.
- Ippolito, L.J.** (1978), "Rain Attenuation Prediction at 10 to 100 GHz from Satellite Beacon Measurements," Abstract, Record, EASCON '78, September 25-27, Arlington, Va.
- Ippolito, L.J.** (1979), "11.7 GHz Attenuation and Rain Rate Measurements with the Communications Technology Satellite (CTS)," NASA TM 80283.
- Ippolito L.J.** (1986), Radiowave Propagation in Satellite Communications, Van Nostrand Reinhold, New York, p. 88.
- Janes, H.B., **J.T. Collins** and **F.K. Steele** (1978), "A Preliminary Catalog of Programs and Data for 10-100 GHz Radio System Prediction," Off. **Telecomm.** Rpt. 78-141.
- Jorgenson, D.L., **W.H. Klein** and **C.F. Roberts** (1969), "Conditional Probabilities of Precipitation Amounts in the Conterminous United States," U.S. Dept. **Comm.**, Env. Sci. Serv. Ad., Weather **Bur.**, Silver Spring, Md., ESSA Tech Memo **WBTM-T DL-18**.
- Kaul, R.**, **D.V. Rogers** and **J. Bremer** (1977), "A Compendium of Millimeter Wave Propagation Studies Performed by NASA," ORI Final Report, prepared under NASA Contract NAS5-24252.
- Kheirallah, H.N.**, **J.P. Knight**, **R.L. Olsen**, **K.S. McCormick** and **B. Segal** (1980), "Frequency Dependence of Effective Path Length in Prediction of Rain Attenuation Statistics," Electr. Letters, Vol. 16, No. 12, pp. 448-450.
- Laws, **J.O.** and **D.A. Parsons** (1943), "The Relation of Raindrop-Size to Intensity," Am. Geophys. Union Trans., Vol. 24, pp. 274-276.
- Lin, **S.H.** (1973), "Statistical Behavior of Rain Attenuation," B.S.T.J., Vol. 52, No. 4, pp. 557-581.
- Lin, **S.H.** (1977), "Nationwide Long Term Rain Rate Statistics and Empirical Calculations of 11 GHz Microwave Rain Attenuation," B.S.T.J., Vol. 56, No. 9, pp. 1581-1604.
- Lin, **S.H.** (1978), "Empirical Calculation of Microwave Rain Attenuation Distributions on Earth-Satellite Paths," Record, EASCON '78, Arlington, Va., pp. 372-378.
- Lin, **S.H.**, **H.J. Bergmann**, and **M.V. Pursley** (1980), "Rain Attenuation on Earth-Satellite Paths - Summary of 10-Year Experiments and Studies," BSTJ, Vol. 59, No. 2, pp. 183-228.

- Marshall, **J.S.** and **W.M. Palmer (1948)**, "The Distribution of Raindrops With Size," Jrnl. Meteorology, vol. 51, pp. 165-166.
- Olsen, **R.L.**, **D.V. Rogers** and **D.B. Hedge (1978)**, "The aR^b Relation in the Calculation of Rain Attenuation," IEEE Trans. Ant. Prop., Vol. **AP-26**, pp. 318-329.
- Oort, **A.H.** and **E.M. Rasmussen (1971)**, "Atmospheric Circulation Statistics," NOAA Professional Paper No. 5, U.S. Dept. Commerce.
- Persinger, **R.R.**, **W.L. Stutzman**, **R.E. Castle** and **C.W. Bostian (1980)**, "Millimeter Wave Attenuation Prediction Using a Piecewise Uniform Rain Rate Model," IEEE Trans. Ant. Prop., Vol. **AP-28**, No. 2, pp. 149-153.
- Rice, **P.L.** and **N.R. Holmberg (1973)**, "Cumulative Time Statistics of Surface Point Rainfall Rates," IEEE Trans. Comm., Vol. **COM-21**, No. 10, pp. 1131-1136.
- Rogers, **D.V.** and **G. Hyde (1979)**, "Diversity Measurements of **11.6-GHz** Rain Attenuation at Etam and Lenox, West Virginia," Comsat Tech. Rev., Vol. **g**, No. 1, pp. 243-254.
- Rogers, **R.R.** (1972), "Radar-Derived Statistics on Slant-Path Attenuation at **10 GHz**," Radio Science, Vol. 7, No. 6, pp. 631-643.
- Saleh, **A.A.M.** (1978), private communication.
- Setzer, **D.E.** (1970), "Computed Transmission Through Rain at Microwave and Visible Frequencies," B.S.T.J, Vol. **49**, No. 8, pp. 1873-1892.
- Skerjanec, **R.E.** and **C.A. Samson (1970)**, "Rain Attenuation Study for 15 GHz Relay Design," NTIS, AD-709-348, Springfield, Va.
- Steele, **F.K.** (1979), private communication.
- Stutzman, **W.L.**, and **Dishman (1982)**, "A simple model for the estimation of rain-induced attenuation along earth-space paths at millimeter wavelengths," Radio Science, Vol. **17**, pp. 1465-1476.
- Stutzman, **W.L.**, and **Dishman (1984)**, Correction to "A simple model for the estimation of rain-induced attenuation along earth-space paths at millimeter wavelengths," Radio Science, Vol. **19**, p. 946.

Stutzman, W.L., and Yen, K.M. (1986), "A Simple Rain Attenuation Model for Earth-Space Radio Links Operating at 10-35 **GHz**," Radio Science, Vol. 21, NO. 1, pp. 65-72.

U.S. Dept. of Commerce, "Telecommunications Analysis Services - Reference Guide," National Telecommunications and Information Agency, Institute for Telecommunications Sciences, Spectrum Utilization Division, 325 South Broadway, Boulder, CO, 80303, June 2, 1981.

Vogel, **W.J.** (1982), "Measurement of Satellite Beacon Attenuation at 11.7, 19.04, and 28.56 GHz and Radiometric Site Diversity at 13.6 **GHz**," Radio Science, Vol. 17, No.6, pp. 1511-1520.